University of Padova

Department of Mathematics

Master Thesis in Data Science

New Risk Measures: Magnitude and Propensity Approach

Supervisor
Professor Martino Grasselli
University of Padova

Co-supervisor
Doctor Michele Bonollo
iason ltd.

Master Candidate
Havva Nilsu Öz

Academic Year
2022-2023

This thesis is dedicated to my family.
For their endless love, support and encouragement

Abstract

Risk measurement, an interdisciplinary field that incorporates probabilistic modeling, data analysis, algorithmic efficiency, and financial markets, is a critical aspect of modern risk management. Traditional risk measures such as Value at Risk and Expected Shortfall offer a single deterministic value representing the potential losses in a given distribution. However, these one-dimensional risk measures may not adequately capture the complexity of real-world risks.

This research investigates the integration of magnitude and propensity in risk analysis to improve risk assessment and decision-making processes. The objective is to develop a comprehensive framework that combines these two key dimensions to provide a more detailed perspective on risk management, i.e., transforming the continues risk distribution to a three point distribution. Real-world data and experiments are analyzed to contribute to the advancement of risk measurement and evaluation practices. By offering a more detailed and robust characterization of risk, the proposed three-dimensional magnitude-propensity approach has the potential to improve risk management practices across various domains.

Contents

Listing of figures

Listing of tables

Listing of acronyms

VaR . . . . . Value at Risk

ES . . . . . Expected Shortfall

P&L . . . . . Profits and Losses

ETCs . . . . . Exchange-Traded Commodities

ETFs . . . . . Exchange-Traded Funds

CIUs . . . . . Collective Investment Undertakings

NAV . . . . . Net Asset Value

EDA . . . . . Exploratory Data Analysis

KDE . . . . . Kernel Density Estimate

CDF . . . . . Cumulative Distribution Function

PDF . . . . . Probability Density Function

1 Introduction

1.1 Background and motivation

Traditionally risk has been defined as the uncertainty concerning occurrence of a loss, see [33]. However there is no single definition of it and different fields can have their own concept of risk. At this point risk management is needed to deal with these uncertainties. Risk management represents a strategic and systematic approach to identify, assess, and respond to potential risks (see [8]). In the field of risk management, a comprehensive and effective process includes several crucial steps that collectively ensure the resilience and stability of an organization, see e.g. [33]. While some steps, including risk identification and management, rely on domain-specific knowledge and organizational expertise, the risk measurement is a highly technical task. The creation of probabilistic models for the unexpected events, the statistical calibration of model parameters, the selection of relevant risk measures, the configuration of their parameters, and the estimation of risk measures based on the data are all part of this task.

In this context, risk measures are essential for quantifying and understanding the level of potential risk exposure. Finding representations that effectively capture the randomness of business variables makes the choice of risk measurements an interesting conceptual problem. For these measurements to provide useful insights into the risks involved, they must meet both quantitative and qualitative criteria (see e.g. [25]). Given the important role of risk measures, significant research efforts have been made in this area, motivated by both academic research

and real-world applications of finance, see e.g. [6]. The financial sector, characterized by strict regulations, has been particularly careful in establishing appropriate risk measures. Governments, central banks and banking regulators have consistently worked to develop reliable risk indicators that reveal banks' risk exposures to market participants and stakeholders.

Figure 1.1: Simplified Risk Management Strategy

Coherent risk measures has become a key factor in the attempt to improve risk assessment. They fulfill a set of characteristics to ensure their reliability and relevance in quantifying risk, see [13]. The criteria for defining the ideal risk measure are shaped by this concept, leading to a richer conceptual understanding of risk assessment.

While traditional risk measurement techniques, such as Value-at-Risk and Expected Shortfall, have provided useful information for risk assessment, finding a more comprehensive and multidimensional risk representation has led to the development of innovative methods (see [27]). One notable development is the quantization approach which requires the estimation of a continuous random variable by a discrete equivalent. Faugeras and Pagès's specifically work on the magnitude-propensity approach which emphasizes the magnitude and probability of losses, see [15]. They introduce Two Point Distribution that represents the continuous risk distribution in which one point represents no loss with the probability $1-p$ and the other point represents the risk m with the probability p. This research aims to implement the introduced method and extending it by implementing constraints. Then to create more comprehensive risk measure which captures more details from the risk distribution, we will introduce Three Point Distribution.

1.2 Literature Review of Risk Measurement and Risk Quantization

We will take a closer look on traditional risk measurement and quantization methods to create a solid background. Every approach considered in this review keeps contributing the modern risk assessment. However the limitations of each approach will be also mentioned to understand the need of the more comprehensive measurement. To understand the characteristics of a good risk measure we should start by defining it.

Definition 1.1. *Let Ω be a sample space and $X : \Omega \to \mathbb{R}$ be the profit or loss variable, risk, associated with a given investment, over a single period of time 0 to t. Then consider a probability space $(\Omega, \mathbb{P})$ and let $\mathbb{X}$ be the set of all risks. A risk measure is a function (see [7]):*

$$\rho : \mathbb{X} \to \mathbb{R} \tag{1.1}$$

Desirable characteristics of risk measures includes several key aspects that are important for their effective application in risk management. Firstly, a risk measure should have intuitiveness which means it should align with a comprehensible notion of risk, such as unexpected losses. This intuitive quality helps in transporting the measure's importance to decision-makers.

Stability is also an essential characteristics of a risk measures. We will see the importance of stability in the results of our experiments in the Section 3. A robust risk measure should show resilience to minor changes in model parameters and should not yield drastic shifts in the estimated loss distribution, see [10]. Additionally, when re-running simulations to generate loss distributions, the risk measure should remain reasonably consistent. It should avoid to have an unreasonable sensitivity to minor alterations in underlying model assumptions.

Thirdly, computational ease is a practical consideration. A risk measure should be computationally efficient, ensuring that its calculation doesn't impose undue complexity (see [10]). More complex risk measures should only be chosen when demonstrable improvements in accuracy outweigh the added computational burden.

Moreover, comprehensibility is vital for senior management's understanding. A risk measure should be transparent and easily understood by senior executives, ideally linked to well-known risk measures that already influence the bank's risk management practices (see [10]). Without this understanding, its impact on daily risk management and business decisions may

be limited. In this research we're comparing the new risk measure we created with the most traditional Value-at-Risk.

Coherence is another important attribute. The risk measure should hold to certain conditions, including monotonicity, positive homogeneity, translation invariance, and subadditivity. Of particular interest is subadditivity, ensuring that the measure appropriately accounts for diversification, a crucial aspect of portfolio risk assessment (see [6]).

Definition 1.2. *Let the risk measure ρ be defined as the Definition 1.1. Then we have the following axioms to define a risk measure as coherent, accordingly to Artzner et al., see [6].*

1. ***Subadditivity:*** *For any pair of loss variables $x_1, x_2 \in \mathbb{X}$,*

$$\rho(x_1 + x_2) \leq \rho(x_1) + \rho(x_2) \tag{1.2}$$

2. ***Monotonicity:*** *If, for all $x_1, x_2 \in \mathbb{X}$ with $x_1 > x_2$, then*

$$\rho(x_1) \geq \rho(x_2) \tag{1.3}$$

3. ***Homogeneity:*** *For any constant $\lambda > 0$ and random loss variable $x \in \mathbb{X}$,*

$$\rho(\lambda x_1) = \lambda \rho(x_1) \tag{1.4}$$

4. ***Translational invariance:*** *For any constant $d \in \mathbb{R}$ and random loss variable $x \in \mathbb{X}$,*

$$\rho(x + d) = \rho(x) + d \tag{1.5}$$

Finally, meaningful risk decomposition is also an essential characteristic. A valuable risk measure should be decomposable into smaller units, allowing risk to be allocated to exposures. Furthermore, it should accurately distribute diversification effects among these components, providing meaningful information for daily risk management practices (see [10]).

1.2.1 Value-at-Risk

Value-at-Risk, a fundamental component of risk management, provides a quantitative estimate of the possible loss an investment or portfolio may encounter over a defined time horizon. Due to its ability to reduce complicated risk scenarios to a single point of reference, VaR is a widely

used risk measure (see [25]). This makes it important for decision makers seeking to identify and mitigate risks from adverse consequences.

Mathematically, VaR is defined as the threshold value beyond which the probability of actual losses exceeding this value is equal to or less than the desired confidence level α (see [21]). Mathematically, VaR can be represented as follows:

$$VaR(\alpha) = \inf \{x \in \mathbb{R} \mid P(X \leq x) \leq \alpha\} \tag{1.6}$$

where the confidence level $\alpha \in (0, 1)$ and $P(X \leq x)$ represents the cumulative probability distribution function of the portfolio's value. The cumulative distribution function gives the probability that the random variable X is less than or equal to x. [30]

VaR is primarily used for risk assessment in many investment strategies and portfolios due to its ability to provide a clear estimate of potential loss, see e.g. [21]. By calculating the maximum loss that could occur under normal market conditions, decision makers will gain a better understanding of the potential negative effects of their investment choices.

However, it is important to note that VaR has its limitations. One noticeable weakness is that it ignores the detailed distribution of losses above the confidence level and instead concentrates only on the size of the potential loss (see [11]). This limitation becomes more obvious in conditions where tail risk or extreme market events are of major concern.

To further illustrate the notion of VaR, consider a practical example. Let's develop a hypothetical dataset capturing the daily returns of a stock over a specified period. The VaR for this dataset will then be computed and displayed.

The density distribution of daily returns is shown by the blue histogram in the resulting the Figure 1.2. The VaR values at different confidence levels are shown as red dashed lines. A VaR of 0.95, for instance, indicates that there is a 5% chance that the portfolio's loss will be greater than that value. This example shows how VaR can be applied to a dataset of stock returns how it offers an understanding of the possible losses of an investment portfolio.

Choosing a confidence level for VaR assessments in practice frequently depends on the investor's or organization's risk tolerance and particular goals. In general 90, 95, and 99 percent confidence levels are being used. A more conservative risk assessment is implied by a greater confidence level, such as 99 percent, which concentrates on capturing extreme tail events that may happen with very low likelihood. Detailed researches has been made into different field's use of confidence interval estimate for VaR, see e.g. [38]. In this research, 99 percent confidence level is used for the VaR calculations in an attempt to provide a comprehensive picture

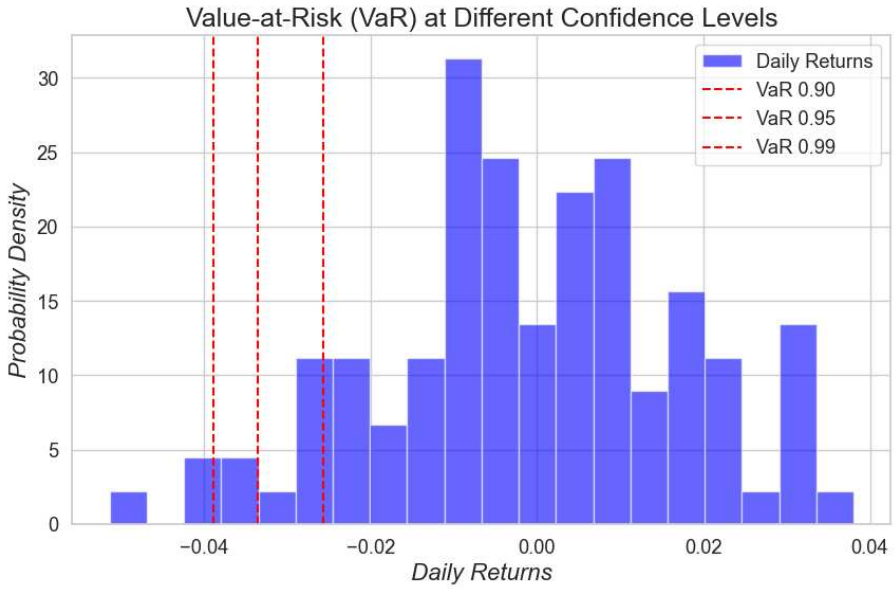

Figure 1.2: Value-at-Risk of the hypothetical dataset

of potential losses while taking into account the worst-case situations.

1.2.2 Expected Shortfall

Expected Shortfall, also known as Conditional Value-at-Risk, has become a popular risk measure in response to VaR's limitations. The estimated value of potential losses that are greater than the VaR level is measured by ES, see [2]. VaR only offers a single-point estimate, whereas ES calculates the average loss above the VaR threshold.

If X is a random variable expressing the risk distribution of a portfolio, then mathematically, ES can be defined as follows:

$$ES(\alpha) = \frac{1}{1-\alpha} \int_{\alpha}^{1} VaR_{\gamma}(X), d\gamma \tag{1.7}$$

where the confidence level $\alpha \in (0, 1)$, $VaR_{\gamma}(X)$ is the Value at Risk at confidence level γ, where $\gamma \in (\alpha, 1)$. Hence the integral calculates the average of VaR values over the tail of the distribution from α to 1, normalized by $(1 - \alpha)$. By considering both the potential amount and probabilities of losses, ES captures the behavior of the loss distribution's tail and offers a more complete measure of risk (see [3]). It gives details on average losses that exceed the VaR threshold as well as the average impact of extreme events.

Elicitability is a mathematical property, satisfied by some risk measures, that allows for the ranking of risk models' performance. If a risk measure is elicitable, then there exists a scoring function for that risk measure that can be used for comparative tests on models. VaR is considered as elicitable but not a coherent risk measure, while ES is a coherent law invariant risk measure but is not elicitable. By law invariant we mean that it assigns the same value to two risky positions having the same distribution with respect to the initial probability measure. However ES is elicitable of higher order in the sense that the pair $(VaR(\alpha), ES\alpha)$ is jointly elicitable, see e.g. [17].

Illustration of the concept of Expected Shortfall with a graphical example is shown in the Figure 1.3. Hypothetical distribution of portfolio losses are generated and then VaR and ES with a 99 percent level of confidence level is calculated.

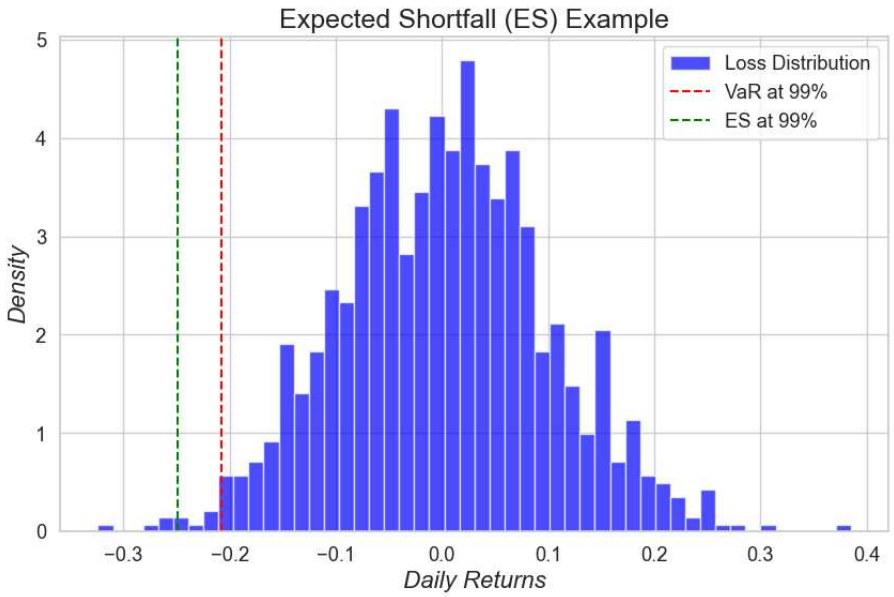

Figure 1.3: Expected Shortfall of the hypothetical dataset

The blue histogram in the Figure 1.3 illustrates the distribution of portfolio losses. The Expected Shortfall at a 99% confidence level is shown by the green dashed line, while the VaR is shown by the red dashed line. A deeper understanding of the potential risks associated with the portfolio is provided by the ES value, which provides information about the average loss above the VaR threshold.

Risk managers are better able to understand the potential risks associated with their portfolio or business by combining VaR and ES. While ES provides additional understanding of tail risk

and the amount of potential loss, VaR helps in setting risk limits and assessing downside risk

1.2.3 Stress Tests

Another important risk assessment tool is stress testing, which allows organizations to determine their resilience to difficult economic conditions and unexpected events. These tests involve putting multiple hypothetical stress scenarios such as market shocks, economic downturns, or crisis driven by a single event onto portfolios or financial institutions (see e.g. [16]). The stress tests helps identifying vulnerabilities and measuring potential losses that might be encountered under challenging conditions by imitating these extreme conditions.

Depending on the degree of severity of the stress scenario, multiple confidence levels are commonly used while performing stress testing. A stress test with different confidence level, as mentioned in Var and ES calculations, can be implemented according to the need. Results of stress tests demonstrate an institution's risk exposure, fund adequateness, and overall financial health. The adoption of this risk management tool by financial institutions to ensure effective risk management processes has grown in significance for regulatory compliance. Specifically, stress testing have been crucial for enhancing the financial sector's resilience in following of the 2008 global financial crisis, see [5]. Stress testing enable institutions to establish suitable risk mitigation methods and sustain financial stability in times of instability by modeling severe yet reliable scenarios.

An example is shown in the Figure 1.4 to demonstrate this. We can think about a scenario that we wish to evaluate the robustness of a stock and bond portfolio to a major market shock. We can design a stressful scenario in which the stock market drops significantly,by 20%in a single day. We learn more about the portfolio's behavior under extreme circumstances by applying this stress scenario to it and examining the losses that occur.

The portfolio value under normal circumstances is represented by the blue line in the Figure 1.4, while the value under the stress scenario is represented by the orange line. The deviation between the two lines during the stress period illustrates the potential impact of the extreme market shock on the portfolio.

1.2.4 The Essential Supremum

The essential supremum is another risk assesment tool that we should consider. Before defining the eseential supremum we should understand what supremum is.

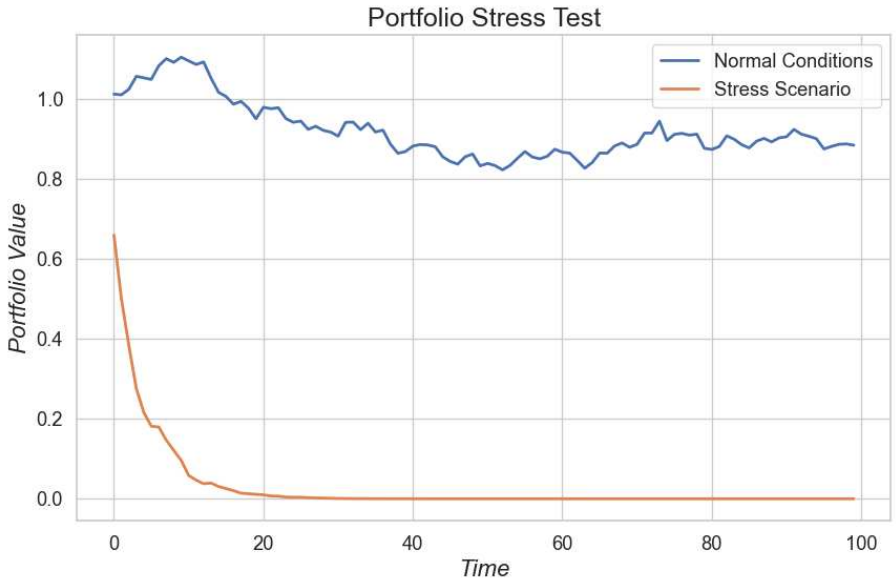

Figure 1.4: Stress Test for hypothetical dataset

Definition 1.3. *Let X be a non-empty set and $f : X \to \mathbb{R}$ be a real-valued function defined on X. The supremum* sup *of the function f over the set X, denoted as* $\sup_X f$*, is defined as follows (see [34]):*

$$\sup_X f := \min\{M \in \mathbb{R} : f(x) \leq M \text{ for all } x\} \tag{1.8}$$

Then we can mathematically define the essential supremum as:

Definition 1.4. *Let X be a non-empty set and $f : X \to \mathbb{R}$ be a real-valued function defined on X. The essential supremum, ess sup, of the function f over the set X, denoted as ess $\sup_X f$, is defined as follows (see [34]):*

$$\textit{ess sup}_X f := \inf\{M \in \mathbb{R} : \mu\{x : f(x) > M\} = 0\} \tag{1.9}$$

where μ is a measure, such as a probability measure, defined over the set X

In other words it's the supremum of a function which holds almost everywhere. The essential supremum is particularly useful when dealing with probability and random variables because it allows us to describe the behavior of random variables without being overly concerned about rare, almost negligible events that might affect the function's values.

For the risk measure we can denote the essential supremum as $\rho_\infty(X)$. As the converse of VaR it quantifies the largest possible loss without revealing any information about the associ-

ated probability (see [29]).

$$\rho_\infty(X) := \operatorname{ess\,sup} X \tag{1.10}$$

The most extreme potential loss is captured by this risk measure, often known as the worst-case scenario or tail VaR, regardless of the likelihood that the event will occur. As a result, it offers a careful estimate of the worst case scenario but fails to offer a comprehensive risk assessment that takes into account both magnitude and propensity factors (see e.g. [12]). One of the main advantages of $\rho_\infty(X)$ lies in its simplicity and ease of interpretation. Risk managers can identify the worst-case scenarios and allocate capital reserves accordingly by concentrating on the largest possible loss. $\rho_\infty(X)$ offers a useful upper bound for risk exposure in scenarios where extreme events may have significant consequences, ensuring that institutions are ready for the worst-case scenarios.

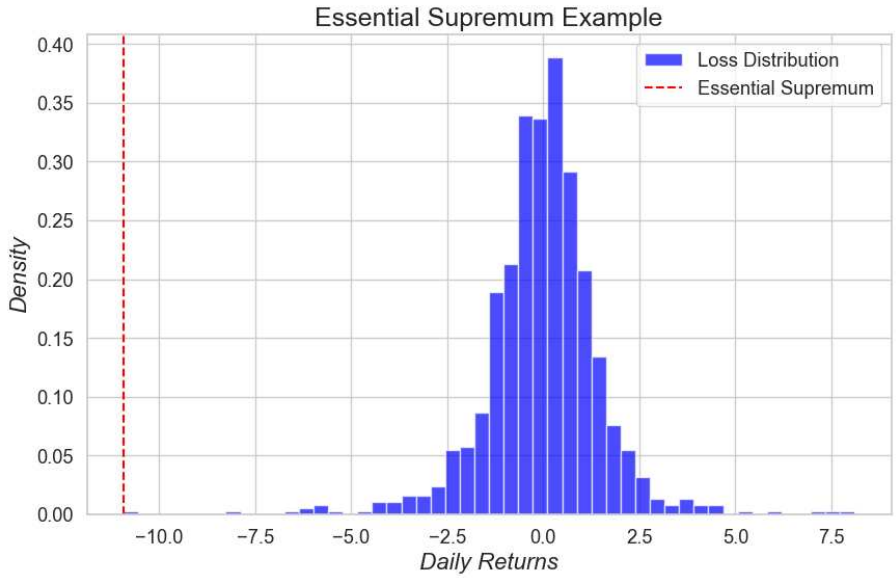

Figure 1.5: Essential Supremum for hypothetical dataset

However, this extreme focus on maximum loss has several impacts. By ignoring probabilities, $\rho_\infty(X)$ neglects the likelihood of less extreme but still significant losses. Risk managers may therefore overlook the effects of moderately severe but more likely events if they simply rely on this measure, resulting in poor risk management techniques. Furthermore, $\rho_\infty(X)$ can be very sensitive to extreme observations and outliers, which makes it vulnerable to estimate errors and model misspecification. For example, financial data frequently displays heavy-

tailed distributions in the real world, which means that extreme events happen more frequently than a normal distribution would have predicted. Therefore, $\rho_\infty(X)$ might overestimate the worst-case scenarios, resulting in inappropriate risk evaluations and a potential overallocation of capital reserves. It's a good example of understanding why we need not only single but multiple dimensinal risk measure and the three point distribution approach aims to fill this gap by giving moderate and extreme risk scenerios with their probabilities.

The blue histogram in the Figure 1.5 illustrates a heavy-tailed loss distribution, which is characteristic of financial data. The largest possible loss in the distribution is represented by the essential supremum, $\rho_\infty(X)$, which is shown as a red dashed line. The essential supremum, unlike VaR or ES, only considers the worst-case scenario and disregards probability.

1.2.5 Risk Quantization

The field of risk analysis' essential area of research, known as risk quantization, has made a significant impact on today's risk management techniques. Given the diversity of risk characteristics, new approaches are needed to better understand and reduce the complexity. Also it is important to overcome the limitations of the risk measures we mentioned in the previous sections. This has led to a many analysis and researches into different approaches which concentrate on the quantization of continuous risk distributions. These efforts has led to a major change in risk management concepts. The two approaches that is used in Faugeras and Pagès's paper are the optimal mass transportation and the optimal quantization.

The optimal mass transportation technique is the problem of finding the most efficient way to move one distribution of objects to match another distribution, while minimizing the cost of transportation (see e.g. [37]). In this research it is based on the idea of reducing the cost that needed to transfer the continuous distribution to the discrete distribution. The transportation cost is defined on some distance metric or cost function, which quantifies the effort or distance required. The Wasserstein distance, used as a measure of dissimilarity between distributions, is an example of optimal mass transportation that our proposed approach is also based on (see [28]).

Definition 1.5. *Let $p \in \mathbb{N}$ and $P, R \in \mathcal{P}_p(\mathbb{R})$ be two probability measures on $\mathbb{R}$ admitting Q_P and Q_R as the quantile functions, respectively. Then, the p-Wasserstein distance between P and R is (see [28]):*

$$W_p(P,R) = \left(\int_0^1 |Q_P(x) - Q_R(x)|^p \, dx \right)^{1/p} \tag{1.11}$$

where Q_P (resp. Q_R) denoted as:

$$Q_P(t) := inf\{x : F_P \geq t\}, 0 < t < 1. \tag{1.12}$$

On the other hand, the optimal quantization technique is the problem of finding a set of discrete points, often referred to as quantization points or centroids, that best represent the original continuous distribution (see [18]). The technique origins in the engineering and signal processing literature, see e.g. [36] and [23]. It aims to reduce the number of quantization levels while keeping as much information as possible to maintain the general structure of the distribution. This research is also based on the Faugeras and Pagès's (see [15]) optimal quantization problem. It is defined as the constrained two-points quantizer with centers $\{x_0, x_1\} := \{0, m\}$, i.e. as a mapping $T : \mathbb{R}^+ \to \{0, m\}$ with

$$T(x) = \begin{cases} m & x \geq a \\ 0 & x < a \end{cases}, \tag{1.13}$$

where a is a threshold to determine. Then, the optimal quantization problem for $X \sim P^X$ with constrained knot at zero writes

$$\inf \mathbb{E}[(X - T(X))^2], \quad a, m \in \mathbb{R}^+ \tag{1.14}$$

where $\mathbb{E}$ represents the expected value which measures the average of possible outcomes taking into account their probability. From Gersho and Gray's work paper introduces a distortion function,

$$L(m) := \mathbb{E}\left[X^2 \wedge (X - m)^2\right]. \tag{1.15}$$

For the three point quantizer we create centers $\{x_0, x_1, x_2\} := \{0, m_1, m_2\}$, i.e. as a mapping $T : \mathbb{R}^+ \to \{0, m_1, m_2\}$ with

$$T(x) = \begin{cases} m_1 & x \geq b \\ m_2 & x \geq a \text{ and } x < b \\ 0 & x < a \end{cases}, \tag{1.16}$$

Then we can write the distortion function for three point quantizer as,

$$L(m_1, m_2) := \mathbb{E}\left[X^2 \wedge (X - m_1)^2 \wedge (X - m_2)^2\right]. \tag{1.17}$$

1.3 Research objectives

The research objectives are intended to improve understanding and use of the propensity-magnitude method to risk measurement. The following are the specific objectives:

- Extension of the Propensity-Magnitude Approach: The main goal is to extend the existing two-dimensional propensity-magnitude framework to three-dimensional cases. By integrating an additional dimension, the study aims to provide a more complete and refined representation of risk. This extension will involve the development of a robust methodology and computational techniques to effectively summarize and quantify the risk in a multidimensional framework.
- Analyzing Large Data Examples: Analyzing big data sets that contain simulated profits and losses produced from real-world scenarios is another objective. The research aims to provide useful information into the performance, accuracy, and applicability of the suggested magnitude-propensity risk measure in practical scenarios. This analysis will offer empirical proof of the approach's efficiency and potential value in risk management.
- Development of Prototypes: The research will involve creating a prototype with the appropriate technology, Python. This prototype will serve as concrete examples of the theoretical framework, proving its feasibility and usefulness in realistic situations.

By fulfilling these objectives, this research will improve the knowledge of the propensity-magnitude technique and its use in multidimensional risk assessment.

1.4 Introduction to the magnitude-propensity framework

Measuring and quantifying risk is important in many areas such as banking and insurance. Risk measures have historically concentrated on capturing the uncertainty and potential losses connected to specific events or scenarios, see e.g. [1]. However, frameworks such as the magnitude-propensity method, that is introduced in Faugeras and Pages' paper, have been developed in response to the need for a more comprehensive and nuanced approach to risk assessment.

The magnitude-propensity approach takes into account the fact that losses and risks can be divided into two categories based on their corresponding magnitudes and propensities. Propensity denotes a likelihood or probability of incurring such a loss, whereas magnitude denotes the severity or size of a possible loss. The magnitude-propensity approach offers a more complete view on risk assessment by taking into account both dimensions simultaneously.

The magnitude-propensity approach addresses the limitation of traditional risk measures by shifting from a one-dimensional representation to a two-dimensional framework (see [15]), where the entire P&L distribution is summarized by a binomial distribution Bin(p), representing the probability (p) of incurring a loss of magnitude (m) and the probability (1-p) of no losses.

A mass problem or an optimal quantization discretization can be used to formulate the problem in order to find the optimal values (m, p) that best represent a given P&L distribution. Finding the binomial distribution that minimizes the difference between the original P&L distribution and the quantized representation is the goal.

The idea of risk due to large magnitudes and risk due to high propensities is another essential idea within the magnitude-propensity framework. A profound understand of how risk emerges across various dimensions is introduced by this idea. While risk due to high propensities captures the likelihood of frequent but relatively small losses, risk due to high magnitudes captures the potential effect of significant losses. When analyzing stochastic ordering, comparing various risks, and taking into account single risk variables, this dual nature of risk becomes clear.

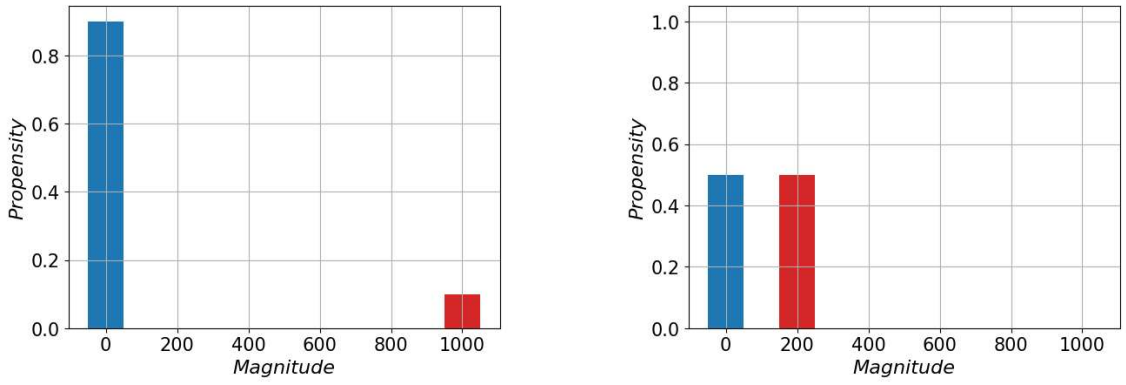

(a) Example 1: X_1 has high magnitude risk

(b) Example 2: X_2 has high propensity risk

Figure 1.6: Intrinsic magnitude-propensity aspect for a single random risk

Let's look at two discrete measures to illustrate this duality: X_1 and X_2. X1 has a 'high'

magnitude risk with a 'low' propensity, $P(X_1 = 1000) = 0.1$ and $P(X_1 = 0) = 0.9$, whereas X2 exhibits a 'small' magnitude risk with a 'high' propensity, $P(X_2 = 200) = 0.5$ and $P(X2 = 0) = 0.5$. Furthermore, X1 and X2 demonstrate the varying implications of magnitude and propensity on the overall risk profile despite sharing the same mean. This idea is illustrated visually in the Figure 1.6, which emphasizes how observing risk from the magnitude-propensity framework offers a more complete perspective.

The importance of the magnitude-propensity approach is further strengthened by this intrinsic understanding of risk dualities.

1.5 Previous studies on risk quantization and real-case examples

Researchers and professionals searching to increase the accuracy and quality of risk measurement have given the field of risk quantization a lot of attention. The different applications of risk quantization in different industries, including as insurance, operational risk, and healthcare, have been investigated in a number of previous studies. These studies have provided understanding on the advantages and practical implications of using a quantized approach to risk assessment. We will give a couple of example that is related to magnitude and propensity approach.

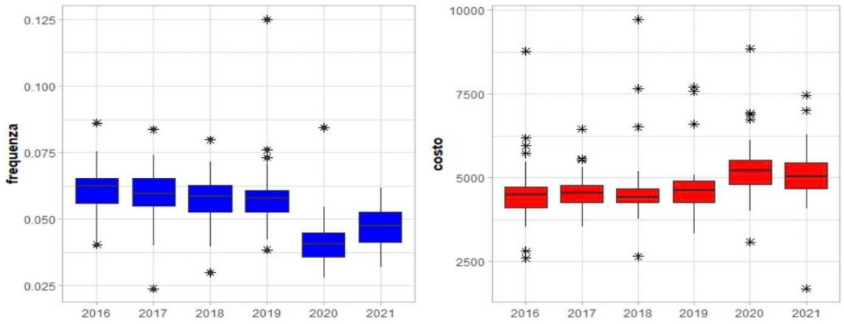

Figure 1.7: Frequency and Cost independently in "Bollettino Statistico"

Risk quantization has been shown to be helpful in the insurance industry for increasing the accuracy of calculations and policy pricing. Insurance firms can more accurately evaluate the risk associated with insuring specific events or assets by estimating the severity and frequency

of potential losses. For instance, the study of the "Bollettino Statistico" in the Italian car insurance sector often reports the claims by taking into account both frequency and severity (see [26]). In the Figure 1.7 and the Figure 1.8 shows the frequency and cost graphs that was shown in the report. The analysis predicts that claim frequency would partially increase in 2021, while average claim expenses will remain stable. By investigating the frequency and severity of claims, this example demonstrates how actuarial models support insurers in risk assessment and management. These insights are crucial for pricing and overall profitability.

Figure 1.8: Frequency and Cost analysis together in "Bollettino Statistico"

In the field of insurance, frequency is based on observable frequencies, whereas severity is frequently indicated by the average (or median) amount of claims. While the severity-frequency framework and our magnitude-propensity approach are similar, there is a key difference to be indicated. Empirical averages are used in traditional insurance policies to measure severity. Our method based on Faugeras and Pages' paper, however, goes a step beyond that. We aim to minimize information loss with respect to the continuous distribution by using a discretization technique, resulting in a more precise representation of risk. This focus on minimizing information distortion enables us to gain complex information and improve our capacity for risk assessment.

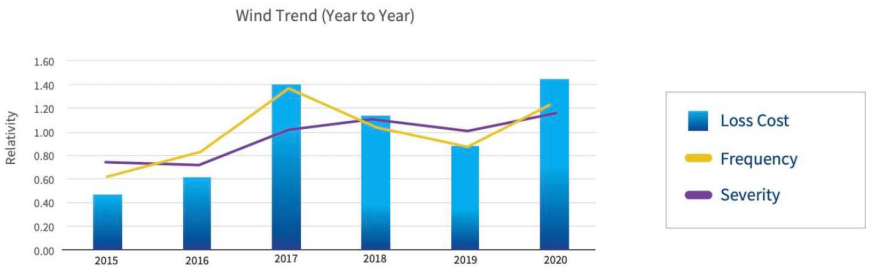

Figure 1.9: LexisNexis: Wind Peril Trend

LexisNexis Risk Solutions is yet another example from the insurance industry. It is a respectable business known for providing comprehensive and trustworthy data-driven insights in the insurance sector. The LexisNexis U.S. Home Insurance Trends Report (see [22]), their annual publication, offers useful details on peril trends in the house insurance sector. The Figure 1.9 and the Figure 1.10 are from the report's 2021 edition, which provides updated and detailed information on loss cost, frequency, and severity for various perils.

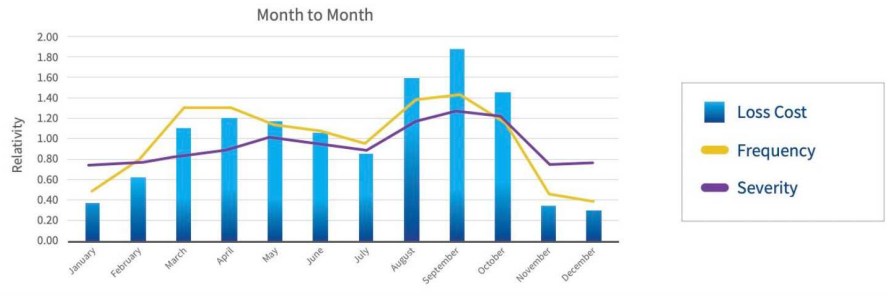

Figure 1.10: LexisNexis: Wind Peril Six-Year Average Seasonality

In the report, frequency and severity are key factors in assessing the impact of perils, such as wind, on the home insurance industry. The frequency of wind-related claims per exposure indicates how frequently the homeowners experience losses due to wind-related events. While severity measures the average amount paid for wind-related claims, severity offers insights into the financial impact of these events. Insurers are able to better understand the risks involved with wind-related losses, modify their prices and assessing strategies, and create efficient risk management plans by examining the frequency and severity patterns of wind peril.

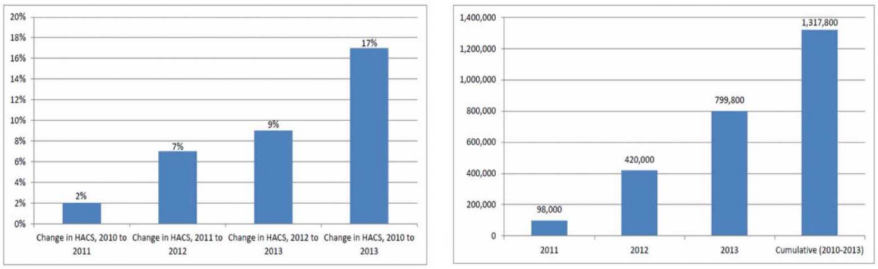

Figure 1.11: Annual and Cumulative HACs

Risk quantification has been used in the healthcare industry to enhance patient safety and optimize resource allocation. Healthcare professionals can prioritize interventions and allocate resources to areas with higher risk profiles by measuring the frequency and severity of negative

events. The report by the Agency for Healthcare Research and Quality (see [4]) in the United States provides an illustration of this type of analysis that is shown in the Figure 1.11. The report offers details on healthcare quality, including measures related to patient safety. The Hospital-Acquired Condition (HAC) rate, which measures the frequency of adverse events that happen during a hospital stay, is one of the metrics implemented. By giving each HAC a weight or impact based on its clinical importance, severity is measured. These weights are used to determine the overall severity of patient safety events inside a hospital and represent the potential impact on patients.

These previous studies highlight the usefulness and advantages of risk quantification across various kinds of fields. As we continue our research on the magnitude-propensity approach, we will build upon the findings and methodologies of these previous studies.

2

Dataset and Methodology

The Dataset and Methodology chapter of this thesis explores the data collection process and the analytical methods utilized in our research. It aims to provide a complete understanding of the dataset and the methodology employed for creating and analyzing risk measures. In this and the following sections the symbol F represents the cumulative distribution, Q denotes the quantile function and f denotes the probability density function of the given distribution. $\mathbb{E}$ denotes the expected value, Var denotes the variance. Also $\mathbb{E}[X^2] < \infty$ means the random variable X has a finite second moment, allowing for well-defined statistical measures like variance.

2.1 Data collection and analysis methods

Before explaining the dataset we should take a look at some preliminaries about P&L Distribution and Risk Factors.

2.1.1 P&L Distribution

We use a space of probabilities to symbolize the uncertainty over how the world will evolve. Consider a particular portfolio, such as a collection of stocks, a financial derivatives, a collection of loans, or even the overall risk profile of a financial institution. In the risk management framework, V_t denotes the portfolio's value at time t. So we assume that this random variable is observable at time t. If we look for a time perspective at t and consider the time period $[t, t+1]$,

then the value V_{t+1} is unknown to us. The distribution of $(V_{t+1} - V_t)$ is called Profit and Loss so it refers to the possible changes in the value of a portfolio over a specific time period, see [25]. We can denote the P&L by

$$L_{t+1} = -(V_{t+1} - V_t) \tag{2.1}$$

The new P&L defined in (2.1) makes losses a positive number and profits negative. In this research we will also indicate losses as positive number during some graphical illustrations in the Section 3 for the sake of simplicity.

2.1.2 Risk Factors

We can model the V_t, the value of the portfolio, as a function of time and set a d-dimensional random vector $\mathbf{Z_t} = (Z_{t,1}, Z_{t,2}, \ldots, Z_{t,d})\prime$ of risk factors. Then we can write,

$$\mathbf{V}_t = g(t, \mathbf{Z}_t), \quad \text{where } g : \mathbb{R} \times \mathbb{R}^d \to \mathbb{R} \tag{2.2}$$

Equation (2.2) characterizes the portfolio's value as a mapping that evolves over time in response to the risk factors such as prices of financial assets, yields or exchange rates.

Considering a fixed holding period, the portfolio's P&L can be defined as the change in the portfolio's value (see [25]), driven by the series of risk factor changes $(\mathbf{X}_t)_{t\in\mathbb{N}}$ where

$$\mathbf{X}_t \coloneqq \mathbf{Z}_t - \mathbf{Z}_{t-\Delta} \tag{2.3}$$

Combining the equations (2.2) and (2.3), the portfolio's P&L distribution at a given time horizon Δ is given by:

$$P\&L_{[t,t+\Delta]} = g(t + \Delta, \mathbf{Z}_t + \mathbf{X}_{t+\Delta}) - g(t, \mathbf{Z}_t) \tag{2.4}$$

In other words, P&L distribution consists in the range of potential profits and losses,denoted as X, that a portfolio may experience over a specific time horizon. Therefore, estimating the Cumulative Density Function of the P&L is the main part of measuring the risk of a portfolio.

$$F(X) = P(X \leq x) \tag{2.5}$$

2.1.3 Historical Simulation

Risk evaluation is an important focus in financial analysis. Historical simulations and Monte Carlo simulations, are important techniques for estimating portfolio volatility over a specific period of time. Historical Simulation assumes that the distribution of changes in value of today's portfolio can be simulated by making draws from the historical time series of past changes, see [31].

Specifically Value-at-Risk defined in the Section 1.2.1, a measurement of possible losses in an investment portfolio or the positions of financial institutions, is frequently calculated through historical simulation. This non-parametric method simulates potential portfolio losses over a specified time horizon using historical data on risk factor returns, see e.g. [20]. In this research historical simulation technique will be used to calculate VaR. It's worth noting that the ultimate goal of VaR models in risk management is to provide a robust estimate or forecast of the P&L distribution, even though the actual P&L distribution is unknown. The historical simulation approach is founded on the assumption that the most recent historical returns of risk factors offer a reliable estimation of their distribution, whether or not time decay coefficients are applied. Consequently, in this approach, these returns are plugged in to the current portfolio, revalued through appropriate pricing functions, to derive the 1-day distribution of the portfolio's P&L. Furthermore, while some banks may choose to employ 500 days of historical data, 250 days represent the minimum regulatory requirement. This choice may vary based on specific institutional practices and regulatory guidelines. These 250 scenarios are subsequently applied to revalue the current portfolio under each scenario, following a predefined formula. This process concludes with the creation of an empirical Profit and Loss distribution, characterized by 250 observations, performing as a valuable resource for risk assessment.

2.1.4 Dataset

10-month long daily P&L time series employed as the basis for implementation of the quantization approach. The specific details of the data used are as follows:

- Perimeter: The Regulatory VaR was calculated for a specific perimeter, focusing on the portfolio. The calculation was limited to the risk factors validated by the Regulator, ensuring compliance with regulatory requirements (see [9]).
- Portfolio: We focused on the portfolio of a major Italian bank for the analysis. This portfolio served as the basis for calculating the Regulatory VaR and evaluating the associated risk.

- Time Window: The time series ranged a period of 194 business days, starting from August 9^{th}, 2022, and ending on May 10^{th}, 2023. This time frame provided a sufficient time for capturing and analyzing the daily P&L data.

The methodology for calculating the loss distribution underlying the Regulatory VaR was based on the full re-evaluation of positions using historical simulation of the risk factors as mentioned in the Section 2.1.3. It is important to note that the Regulatory VaR calculation had some variations compared to the similar measures calculated for management purposes. These differences are essential to ensure compliance with regulatory guidelines and focus the analysis on relevant factors for regulatory reporting.

Unlike other forms of VaR, such as Gestional VaR, which is adapted towards internal management and strategic decision-making, the primary goal of Regulatory VaR is to ensure that banks hold adequate capital reserves to cover potential losses under adverse market conditions. The application of Regulatory VaR is limited to the prudential portfolio and risk factors specifically validated by the regulator. This restriction ensures that the analysis meets requirements and focuses on factors deemed critical for regulatory purposes, see [24].

The Profit and Loss data used in the VaR distribution is equally weighted, meaning that a decreasing weight over time was not applied. This simplified approach enables a straightforward calculation and analysis of P&L data, avoiding the introduction of additional weighting considerations.

In the risk analysis conducted, the focus was on specific risk factors that had been validated and approved by regulatory authorities as of September 30^{th}, 2020 (see [14]). These validated risk factors contains a wide range of elements, including generic risk on interest rates, generic and specific risk on debt and equity instruments, as well as exposure to commodity-related risks. In addition, the analysis take into account the risk associated with positions in financial instruments such as ETCs (Exchange-Traded Commodities), ETFs (Exchange-Traded Funds), and CIUs (Collective Investment Undertakings) with daily Net Asset Value (NAV). By focusing the analysis on these validated risk factors, the approach ensures the compliance with regulatory guidelines and focuses on the elements that are considered significant for prudential risk management.

2.2 Data Preprocessing and Exploratory Data Analysis

On the provided dataset of daily P&L values, an extensive procedure of data preprocess and exploratory data analysis was carried out in order to get useful insights and make informed decisions. This crucial preliminary phase lays the foundation for the subsequent analytical steps by ensuring data quality, identifying patterns, and uncovering potential anomalies. Data preprocessing is the process of cleaning, transforming, and organizing raw data into a format that can be analyzed.

Conversely, exploratory data analysis digs deeper into the dataset's descriptive statistics, distributions, and visual representations to uncover hidden relationships and trends. This section provides an detailed description of the stages involved in data preprocessing and EDA, illuminating the conclusions drawn and the choices made in light of the processed data.

2.2.1 Time Series Graph

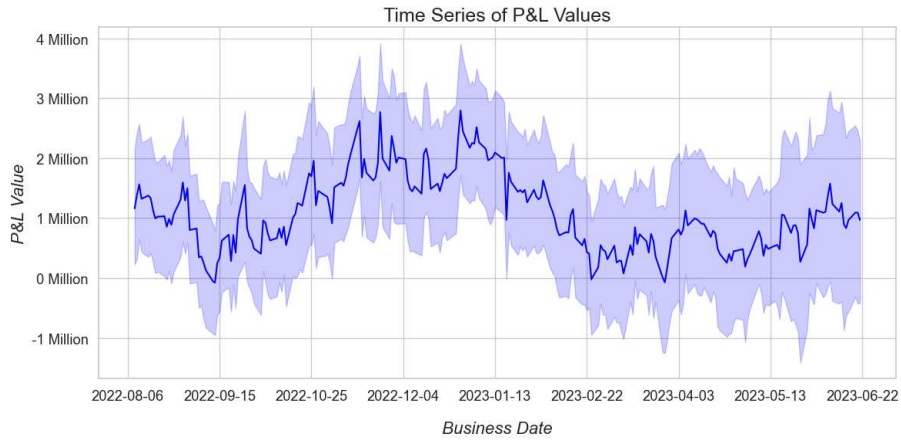

Figure 2.1: Time Series Graph of Profit and Loss Values

The time series graph shown in the Figure 2.1 offers a visual representation of the dynamic changes in P&L values over a period of time. The x-axis corresponds to the business dates, while the y-axis represents the P&L values. It provides a visual representation of the P&L values' temporal distribution, offering a glimpse into the financial performance trends of the organization. The plot indicates the P&L volatility across various business dates. Interestingly we observe a considerable sharp movements in P&L value, indicating a period of exceptional profitability

or loss. This could be attributed to possible reasons, such as market events, strategic decisions, economic factors.

2.2.2 Summary Statistics

The Table 2.1 presents a general overview of the daily P&L values for the observed period. From the statistical results, several of important conclusions can be drawn. The financial performance of the organization is dynamic, as seen by the large day-to-day variation in the mean P&L numbers. Between relatively low values, like around 250,000, and significantly larger values, such over 2,000,000, the mean P&L might change over time implies both periods lower and higher probability. Also some business days mean value ended up being negative, for example the day 13.09.2022, which indicates the loss overcome the profit.

BUSINESS_DATE	count	mean	std	min	max
9.08.2022	250	1,160,637	7,717,980	-28,924,882	34,629,316
10.08.2022	250	1,383,536	8,209,034	-21,554,105	41,479,325
11.08.2022	250	1,562,063	7,444,806	-25,293,732	35,470,560
...	...	...	...	...	...
19.06.2023	251	1,091,564	11,956,690	-31,394,175	42,721,738
20.06.2023	251	1,092,161	11,954,207	-32,632,343	43,715,888
21.06.2023	251	968,470	11,231,436	-31,253,164	43,743,416

Table 2.1: Summary Statistics

Furthermore, it is also important to notice the standard deviation of the P&L values. Higher standard deviation values denote higher volatility and variability in the data points. The high standard deviation is a consequence of days with extremely high or low P&L figures, both in the positive and negative directions. This could indicate that the organization is exposed to a lot of risk and uncertainty, which could make financial planning and forecasting challenging.

The minimum and maximum P&L values provide information about the potential extremes of the business's financial performance. The minimum values, often in the negative range, indicates that days of significant losses, while the maximum values represent days of extraordinary gains. These extremes highlight the potential for both significant obstacles and opportunities within the business operations.

Additionally, it is clear from trends over time that the organization has periods of relative stability followed by unexpected increases or decreases in P&L values. In order to develop strate-

gies to reduce risks and take advantage of advantageous circumstances, it may be important to identify the causes of these fluctuations.

2.2.3 Distribution Analaysis

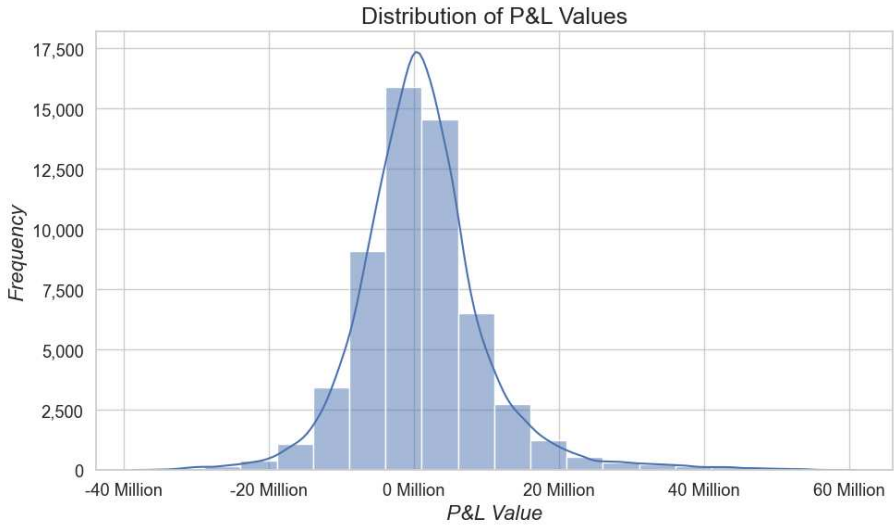

Figure 2.2: Distribution Analaysis of P&L

The Figure 2.2 provides a visual representation of the frequency distribution of P&L (Profit and Loss) values in the dataset. This type of analysis is crucial for gaining insights into the underlying patterns and characteristics of the data.We can determine the range of P&L values that occur most frequently as well as any potential outliers or strange trends by looking at the distribution of these values. The graph's histogram and kernel density estimate plot show the distribution's shape, indicating whether it is symmetric, skewed, or has several peaks.

The overall distribution of the P&L values appears to be skewed and the negative values are generally in the range between 0 to 10 million. As we can see from the largest bin in the Graph 2.2 that the most frequent event is the case of small amount of losses. This asymmetry suggests that the business may encounter more instances of under-performance compared to outstanding success. However when we calculated the skewness, the distribution of P&L values shows a positive skewness of 0.93. This positive skew suggests that there are a few instances of extraordinarily high profits since it shows that the distribution shifts towards greater positive values, which frequently imply that while most transactions yield modest profits, certain particular occurrences or transactions produce disproportionally huge earnings.

2.3 General Idea of Two Point Quantization and the Constraint Experiments

Before explaining the new extension we should understand the two point quantization technique presented by Faugeras and Pagès. The general idea of the magnitude and propensity approach in quantifying risks is to unreveal the magnitude and propensity of a distribution of risks thereby gaining an understanding fuller picture of the underlying risk. It's idea is based on creating a risk measure $\rho(X)$ that can be deterministic representative of the random risk X.

This approach addresses the limitations of risk measures that often mix both the magnitude and propensity the into a single value, resulting in a lack of clarity and understanding of the characteristics of the risk.

The optimal transport approach which is explained in the Section 1.2.5 challenges the constraints of traditional risk measures by reinterpreting them as outcomes of mass transportation from the original risk distribution P^X to a Dirac δ_m measure. Let's define the Dirac measure to be clear on the idea.

Definition 2.1. *Let (X, A) be a measurable space and X be a nonempty set and $x \in X$. Define, for every $A \in \mathcal{P}(X)$,*

$$\delta_x(A) = \begin{cases} 1 & if\, x \in A \\ 0 & if\, x \notin A \end{cases} \tag{2.6}$$

Then, δ_x is a measure in X, called the Dirac measure in x (see [35]).

Such measure is concentrated on the singleton x. This Dirac distribution condenses all risk information into a single point with a magnitude denoted as m, representing both the magnitude and propensity of risk since magnitude m carries full propensity. To address this limitation and provide a more extensive representation of risk, the optimal transport approach proposes a two-point distribution P^Y, which contains both magnitude and propensity aspects (see [15]).

$$P^Y = (1-p)\delta_0 + p\delta_m \tag{2.7}$$

This approach allows for a more explicit representation of risk, where a loss of magnitude m_X occurs with probability p_X, and no loss occurs with probability $(1-p_X)$. The risk measure

is then determined by minimizing the squared Wasserstein W_2 distance between P^X and P^Y, considering a specific set of distributions $\mathcal{A}_0$.

The general definition of Wasserstein function is already given in the Section 1.2.5. We will consider the W_2 version. Now we can define the general problem for two point quantization that is given in Faugeras and Pagès' paper.

Definition 2.2. *Let $\mathcal{A}_0 := \{P^Y = (1-p)\delta_0 + p\delta_m,\ p \in (0,1),\ m \in \mathbb{R}^+\}$, as given in the Definition 2.7, be the set of two-point distributions. For $X \sim P^X$ with $\mathbb{E}[X^2] < \infty$, the bivariate magnitude-propensity risk measure (m_X, p_X) is obtained by minimizing the Wasserstein W_2 distance from P^X to $\mathcal{A}_0$,*

$$(m_X, p_X) = \arg inf_{P^Y \in \mathcal{A}_0} W_2(P^X, P^Y) \tag{2.8}$$

A direct optimization approach can be used to characterize the (m_X, p_X) by using the explicit form of the Wasserstein metric in dimension one: denote by Q_X the quantile function of P_X,

$$Q_X(t) := inf\{x : F_X \geq t\}, 0 < t < 1. \tag{2.9}$$

And the quantile function for $Y \in A_0$ is

$$Q_Y(t) = m\mathbf{1}_{1-p<t\leq 1}. \tag{2.10}$$

Then the following equation can be optimized to get more information about characteristic (see [32]):

$$W_2{}^2(P^X, P^Y) = \int_0^1 (Q_X(t) - Q_Y(t))^2 dt \tag{2.11}$$

for univariate P^X, P^Y with finite variance.

2.3.1 Main objective function with constraint

To extent Faugeras and Pagès's paper we will conduct an experiment by defining constraints to the optimization function. The computation of (m_X, p_X) in the constrained two point distribution involves a minimization process to achieve a representative risk measure that effectively balances both magnitude and propensity aspects of risk. This is achieved through the

optimization of an objective function while considering specific constraints. One crucial constraint imposed on the optimization process is the preservation of the first moment derived from the original loss distribution, within the newly formed two point distribution.

To be more clear we will implement a mean constraint. Since the new distribution will represent the losses, we will take the mean of the negative values of the original distribution. The mean of the negative values in the distribution X, which corresponds to the empirical distribution derived from the daily P&L time series of the bank's portfolio as defined in Section 2.1.4, can be found as:

$$\mathbb{E}[X|X < 0] = \sum_{i=1}^{n} p(x_i).x_i.\mathbf{1}_{x_i<0} = \sum_{i=1}^{n} \frac{x_i \mathbf{1}_{x_i<0}}{k} \tag{2.12}$$

where k is the number of values less than zero which represents the loss since all of the variables in the distribution have the same probability. It is due to the fact that each observation is given equal weight due to their empirical nature. In other words,

$$k = \sum_{i=1}^{n} \mathbf{1}_{X_i<0} \tag{2.13}$$

Since the distribution Y consists of two points $\{0, m_X\}$ with probabilities $\{1 - p_X, p_X\}$, we have the following mean

$$\mathbb{E}[Y] = m_X.p_X + 0.(1 - p_X) = m_X.p_X \tag{2.14}$$

This constraint ensures that the resulting risk measure retains a meaningful connection to the underlying loss data. By constraining the mean of the new distribution to closely align with the mean of the historical loss distribution, the calculated risk measure (m_X, p_X) maintains a consistency with the observed financial loss patterns.

Another important constraint involves both mean and variance. In this case, the objective is to not only preserve the mean of the original loss distribution but also the variance. For the variance again the negative values will be considered so that the variance of the new distribution of the risk and the variance of the losses in the original distribution can be equal. Let X be P&L values as defined in Section 2.1.4, then the variance of the negative values in the original

distribution:

$$\begin{aligned}\text{Var}[X|X<0] &= \sum_{i=1}^{n} p(x_i)\cdot(x_i - \mathbb{E}[X|X<0])^2 \cdot \mathbf{1}_{\{x_i<0\}} \\ &= \sum_{i=1}^{n} \frac{(x_i - \mathbb{E}[X|X<0])^2 \cdot \mathbf{1}_{\{x_i<0\}}}{k}\end{aligned} \tag{2.15}$$

where k is given by the Definition 2.13

The variance of the distribution Y is calculated as:

$$Var[Y] = p_X(m_X - \mathbb{E}[Y])^2 + (1-p_X)(0-\mathbb{E}[Y])^2 \tag{2.16}$$

Incorporating both mean and variance preservation constraints ensures that the risk measure (m_X, p_X) not only captures the historical average loss but also the range of losses around the mean.

2.4 Three point quantization

After gaining information about the new risk measurement, proposed by Faugeras and Pagès, and implementing some experiments on it, we will develop this approach to another level. We aim to extend this proposed two point quantization method to three point discrete distribution. In particular to refine one's measure of risk into a moderate risk and a large risk we will use directly a three points discrete measure,

$$P^Y = (1-p_1-p_2)\delta_0 + p_1\delta_{m_1} + p_2\delta_{m_2} \tag{2.17}$$

where $m_1 < m_2$. With a such three points discrete measure, we can encode and quantify both moderate, resp. large risk, in the magnitude and propensity scale with (m_1, p_1), resp. (m_2, p_2).

Quantile function of the original distribution in the Definition 2.9 still holds in this extension. We can define the quantile function of the three point distribution Y as:

$$Q_Y(t) = m_1\mathbf{1}_{1-(p_1+p_2)<t\leq 1} + m_2.\mathbf{1}_{1-p_2<t\leq 1} \tag{2.18}$$

where $p_1, p_2 \in (0,1)$ and $m_1, m_2 \in \mathbb{R}^+$.

2.4.1 Main objective function

Similar to the two-point quantization, the main objective function in the three-point quantization plays an important role in guiding the selection of the three representative points. A direct optimization approach can again be used to characterize the (m_1, p_1) and (m_2, p_2) by using the explicit form of the Wasserstein metric in dimension one: denote by Q_X the quantile function of P_X, denoted in the above. Then we can define

$$W_2{}^2(P^X, P^Y) = \int_0^1 (Q_X(t) - Q_Y(t))^2 dt \tag{2.19}$$

for univariate P^X, P^Y with finite variance where P^Y is given by the Definition 2.17.

2.4.2 Main objective function with constraint

We will implement a constraint experiment as we did in the two point distribution however this time we will try a different idea. This time we will make m_2 to be as much extreme as it can get by constraining it with VaR.

So we will implement the constraint

$$|m_2| > |VaR| \tag{2.20}$$

By imposing this constraint, the risk measure ensures that the magnitude of the extreme risk m_2 remains greater than the magnitude of the VaR threshold. This constraint highlights the importance of adequately capturing extreme events and the associated potential losses that can have great implications for financial institutions. The requirement (2.20) acknowledges that extreme risks can pose severe systemic consequences and should not be underestimated in risk assessments.

2.4.3 Theoretical analysis

The theoretical analysis of the three-point quantization approach investigates into the mathematical foundations and properties of the methodology. This analysis involves exploring the theoretical ground works of the objective function and the resulting quantized distribution.

By conducting a theoretical analysis, we develop a solid foundation for the approach and gain information about its strengths, limitations, and applicability to various risk quantification scenarios. We will start by implementing the Wasserstein function with the quantile functions we defined in the previous section and try to derive some characterizations, i.e, we will try to achieve necessary and sufficient conditions analysis as Faugeras and Pagès' did in their two point quantization work.

Necessary Conditions Analysis: Let X s.t. $\mathbb{E}[X^2] < \infty$

The squared Wasserstein distance between P^X and $P^Y \in A_0$ writes

$$
\begin{aligned}
{W_2}^2(P^X, P^Y) &= \int_0^1 (Q_X(t) - Q_Y(t))^2 dt \qquad (2.21)\\
&= \int_0^{1-(p_1+p_2)} (Q_X(t))^2 dt + \int_{1-(p_1+p_2)}^{1-p_2} (Q_X(t) - m_1)^2 dt \\
&\quad + \int_{1-p_2}^1 (Q_X(t) - (m_1+m_2))^2 dt \\
&= \int_0^{1-(p_1+p_2)} (Q_X(t))^2 dt + \int_{1-(p_1+p_2)}^{1-p_2} (Q_X(t))^2 dt \\
&\quad - 2m_1 \int_{1-(p_1+p_2)}^{1-p_2} Q_X(t) dt + {m_1}^2 p_1 + \int_{1-p_2}^1 (Q_X(t))^2 dt \\
&\quad - 2(m_1+m_2) \int_{1-p_2}^1 Q_X(t) dt + (m_1+m_2)^2 p_2 \\
&= \mathbb{E}[X^2] + {m_1}^2 p_1 + (m_1+m_2)^2 p_2 - 2m_1 \int_{1-(p_1+p_2)}^1 Q_X(t) dt \\
&\quad - 2m_2 \int_{1-p_2}^1 Q_X(t) dt \\
&:= \psi(m_1, m_2, p_1, p_2)
\end{aligned}
$$

ψ is differentiable and any optimal magnitude-propensity (m_1, p_1) and (m_2, p_2) solving the main objective function must satisfy the first order conditions:

$$\begin{cases} \frac{\partial\psi(m_1,m_2,p_1,p_2)}{\partial m_1} = 0 \\ \frac{\partial\psi(m_1,m_2,p_1,p_2)}{\partial p_1} = 0 \\ \frac{\partial\psi(m_1,m_2,p_1,p_2)}{\partial m_2} = 0 \\ \frac{\partial\psi(m_1,m_2,p_1,p_2)}{\partial p_2} = 0 \end{cases} \Leftrightarrow \begin{cases} 2m_1p_1 + 2(m_1+m_2)p_2 - 2\int_{1-(p_1+p_2)}^{1} Q_X(t)dt = 0 \\ m_1^2 - 2m_1Q(1-(p_1+p_2)) = 0 \\ 2(m_1+m_2)p_2 - 2\int_{1-p_2}^{1} Q_X(t)dt = 0 \\ (m_1+m_2)^2 - 2m_1Q(1-(p_1+p_2)) - 2m_2Q(1-p_2) = 0 \end{cases} \tag{2.22}$$

For $m_1 \neq 0$, $p_1 \neq 0$, $m_2 \neq 0$ and $p_2 \neq 0$, the following results obtained as a necessary conditions:

- From the second and third equation in (2.22), we get:

$$m_1 = 2Q(1-(p_1+p_2)) \tag{2.23}$$

$$(m_1+m_2) = \frac{\int_{1-p_2}^{1} Q_X(t)dt}{p_2} \tag{2.24}$$

- By using the equality (2.24) to solve the first equation in (2.22), we get:

$$m_1 = \frac{\int_{1-(p_1+p_2)}^{1-p_2} Q_X(t)dt}{p_1} \tag{2.25}$$

- By using the equality (2.23) to solve the fourth equation in (2.22), we get:

$$m_2 = 2Q(1-p_2) - 2m_1 \tag{2.26}$$

Sufficiency Condition Analysis: Let X s.t. $\mathbb{E}[X^2] < \infty$.

If P^X has density f such that $f(Q(p)) > 0$, then Q is differentiable with derivative the quantile-density $q_x(p) = Q(p)' = \frac{1}{f(Q(p))}$. Then ψ is twice differentiable with Hessian matrix. The goal is to identify the critical points, such as (m_1, p_1) and (m_2, p_2), where the function reaches local minima or maxima. The Hessian matrix being positive definite at these critical points is important because it ensures the function's second derivative is positive, indicating a local minimum. This helps us to confirm the stability of these points in the analysis.

Since ψ depends on four variables, we will take derivatives with respect to all of these four variables. Because when we are calculating the Hessian matrix, we are examining how small changes in each of these variables affect the function's curvature. Hence the Hessain matrix is:

$$H = \begin{bmatrix} \frac{\partial^2\psi}{\partial m_1^2} & \frac{\partial^2\psi}{\partial m_1 \partial p_1} & \frac{\partial^2\psi}{\partial m_1 \partial m_2} & \frac{\partial^2\psi}{\partial m_1 \partial p_2} \\ \frac{\partial^2\psi}{\partial m_1 \partial p_1} & \frac{\partial^2\psi}{\partial p_1^2} & \frac{\partial^2\psi}{\partial m_2 \partial p_1} & \frac{\partial^2\psi}{\partial p_1 \partial p_2} \\ \frac{\partial^2\psi}{\partial m_1 \partial m_2} & \frac{\partial^2\psi}{\partial m_2 \partial p_1} & \frac{\partial^2\psi}{\partial m_2^2} & \frac{\partial^2\psi}{\partial m_2 \partial p_2} \\ \frac{\partial^2\psi}{\partial m_1 \partial p_2} & \frac{\partial^2\psi}{\partial p_1 \partial p_2} & \frac{\partial^2\psi}{\partial m_2 \partial p_2} & \frac{\partial^2\psi}{\partial p_2^2} \end{bmatrix} = \begin{bmatrix} a & b & c & d \\ b & e & f & g \\ c & f & h & i \\ d & g & i & j \end{bmatrix}$$

with

- $a = 2p_1 + 2p_2$
- $b = 2m_1 - 2Q(1 - (p_1 + p_2)) = 2m_1 - m_1 = m1$ by (2.23)
- $c = 2p_2$
- $d = 2(m_1 + m_2) - 2Q(1 - (p_1 + p_2)) = 2(m_1 + m_2) - m_1 = m_1 + 2m_2$ by the condition (2.23)
- $e = 2m_1 Q'(1 - (p_1 + p_2))$
- $f = 0$
- $g = 2m_1 Q'(1 - (p_1 + p_2))$
- $h = 2p_2$
- $i = 2(m_1 + m_2) - 2Q(1 - p_2) = 2(m_1 + m_2) - (m_2 + 2m_1) = m_2$ by the condition (2.26)
- $j = 2m_1 Q'(1 - (p_1 + p_2)) + 2m_2 Q'(1 - p_2)$

So in the end we have:

$$c = h, f = 0 \text{ and } e = g.$$

Let's modify the matrix accordingly to those equations.

$$H = \begin{bmatrix} a & b & c & d \\ b & e & 0 & e \\ c & 0 & c & i \\ d & e & i & j \end{bmatrix}$$

In order to say that a matrix is positive definite, we should apply a test. Determinant of all $k \times k$ upper-left sub-matrices must be positive. First break the matrix in to several sub matrices, by progressively taking $k \times k$ upper-left elements. If the determinants of all the sub-matrices are positive, then the original matrix is positive definite (see [19]). This test examines whether all possible combinations of k rows and k columns within the matrix yield positive determinants. If every single one of these determinants turns out to be positive, it validates the positive definiteness of the original matrix. Thus each determinant being greater than zero will construct our sufficiency conditions in order to have local minima with the optimal points.

So in our case the Hessian matrix is positive definite at the critical points (m_1, p_1) and (m_2, p_2) if the following conditions are satisfied:

$$|a| > 0 \tag{2.27}$$

$$\begin{vmatrix} a & b \\ b & e \end{vmatrix} > 0 \tag{2.28}$$

$$\begin{vmatrix} a & b & c \\ b & e & 0 \\ c & 0 & c \end{vmatrix} > 0 \tag{2.29}$$

$$\begin{vmatrix} a & b & c & d \\ b & e & 0 & e \\ c & 0 & c & i \\ d & e & i & j \end{vmatrix} > 0 \tag{2.30}$$

Let's calculate the determinants and construct the inequalities one by one.

For the condition (2.27), it is clear that $|a| > 0$ since $p_1 > 0$ and $p_2 > 0$ which implies

$$a = 2p_1 + 2p_2 > 0 \tag{2.31}$$

Since this holds by the definition of p_1 and p_2, we will not consider the inequality (2.31) as a condition.

Let's calculate the second determinant in the condition (2.28),

$$\begin{aligned}\begin{vmatrix} a & b \\ b & e \end{vmatrix} &= a \cdot e - b^2 \\ &= (2p_1 + 2p_2) \cdot (2m_1 Q'(1 - (p_1 + p_2))) - (m_1)^2 \\ &= m_1((2p_1 + 2p_2) \cdot (2Q'(1 - (p_1 + p_2))) - m_1)\end{aligned}$$

Hence the first sufficiency condition is:

$$m_1((2p_1 + 2p_2) \cdot (2Q'(1 - (p_1 + p_2))) - m_1) > 0 \tag{2.32}$$

Now let's check the third determinant in the condition (2.29),

$$\begin{aligned}\begin{vmatrix} a & b & c \\ b & e & 0 \\ c & 0 & c \end{vmatrix} &= a \cdot e \cdot c - b^2 \cdot c - c^2 \cdot e \\ &= c \cdot (a \cdot e - b^2 - c \cdot e) \\ &= c \cdot (e \cdot (a - c) - b^2) \\ &= 2p_2 \cdot (2m_1 Q'(1 - (p_1 + p_2)) \cdot (2p_1 + 2p_2 - 2p_2) - m_1^2) \\ &= 2p_2 \cdot (2m_1 Q'(1 - (p_1 + p_2)) \cdot 2p_1 - m_1^2) \\ &= m_1(4p_1 p_2 \cdot (2Q'(1 - (p_1 + p_2)) - m_1))\end{aligned}$$

Hence the second sufficiency condition is:

$$m_1(4p_1 p_2 \cdot (2Q'(1 - (p_1 + p_2)) - m_1)) > 0 \tag{2.33}$$

Lastly let's take the determinant of the entire matrix:

$$\begin{aligned}\Delta H &= acej - aei^2 + ace^2 + b^2cj + b^2i^2 - c^2ej + c^2e^2 - cd^2e - 2bcei \\ &\quad + 2bcde + 2cdei \\ &= cj(ae + b^2) + i^2(b^2 - ae) + c^2e(e - j) + cei(6b - 2d) + ace^2 \\ &= 32{m_1}^2p_1p_2Q'(1 - (p_1 + p_2))^2 + 32{m_1}^2{p_2}^2Q'(1 - (p_1 + p_2))^2 \\ &\quad + 4{m_1}^3p_2Q'(1 - (p_1 + p_2)) + 16m_1m_2p_1p_2Q'(1 - p_2)Q'(1 - (p_1 + p_2)) \\ &\quad + 32m_1m_2{p_2}^2Q'(1 - p_2)Q'(1 - (p_1 + p_2)) + 4{m_1}^2m_2p_2Q'(1 - p_2) + {m_1}^2{m_2}^2 \\ &\quad - 4m_1{m_2}^2p_1Q'(1 - (p_1 + p_2)) - 20m_1{m_2}^2p_2Q'(1 - (p_1 + p_2)) \\ &\quad + 16{m_1}^2m_2p_2Q'(1 - (p_1 + p_2))\end{aligned}$$

After simplifying the equation we achieve the third sufficiency condition:

$$\begin{aligned}\Delta H &= 4{m_1}^2p_2Q'(1 - (p_1 + p_2))[8(p_1 + p_2)Q'(1 - (p_1 + p_2)) + m_1 + 4m_2] \\ &\quad 4m_1m_2p_2Q'(1 - p_2)[4Q'(1 - (p_1 + p_2))(p_1 + 2p_2) + m_1] \\ &\quad m_1{m_2}^2[m_1 - 4Q'(1 - (p_1 + p_2))(p_1 - 5)] \\ &> 0 \end{aligned} \tag{2.34}$$

The inequalities (2.32), (2.33) and (2.34) we created, represents the sufficiency conditions for (m_1, p_1) and (m_2, p_2) to become an optimal solution.

2.4.4 Quantile Function Experiment

To analyze the effectiveness of the new approach we will implement it on a synthetic data we created. Synthetic datasets are created using different probability distributions, including Uniform, Exponential, and Pareto distributions. We will define the quantile functions of the distributions and solve the neccesary conditions provided in Section 2.4.3. The graphical results of the examples will be shown in the Section 3.2.1.

Definition 2.3. *Let X be a continuous random variable. Then, X is said to be uniformly distributed with minimum a and maximum b, denoted as $X \sim U(a, b)$, if and only if, for any subinterval $[c, d]$ within the range $[a, b]$, the probability of X falling within that subinterval is proportional to the length of the subinterval. In other words, for any values c and d such that $a \leq c < d \leq b$, the probability that X lies in the interval $[c, d]$ is given by:*

$$P(c \leq X \leq d) = \frac{d-c}{b-a} \tag{2.35}$$

This means that all subintervals of the same length within the range $[a, b]$ *have the same probability of occurrence.*

Example 1. *Let* X *be a random variable following a continuous uniform distribution,* $X \sim U(a, b)$*.Then, the quantile function of* X *is (see [36])*

$$Q_X(p) = \begin{cases} -\infty, & \text{if } p = 0 \\ bp + a(1-p), & \text{if } p > 0 \end{cases} \tag{2.36}$$

In the research we will create distribution $X \sim U(0, b)$, which indicates that the $Q(p) = bp$, for the different values of $b = 1, 2, 5, 10$

After we solve the equations (2.23), (2.24), (2.25) and (2.26) for the quantile function $Q(p) = bp$, we get the following solutions:

$$m_1 = 2b(1 - (p_1 + p_2)) \tag{2.37}$$

$$m_1 + m_2 = b - \frac{p_2}{2} \tag{2.38}$$

Definition 2.4. *Let* X *be a random variable. Then,* X *is said to be exponentially distributed with rate (or, inverse scale)* λ

$$X \sim Exp(\lambda), \tag{2.39}$$

if and only if its probability density function is given by

$$E(x; \lambda) = \lambda \exp[-\lambda x], \quad x \geq 0 \tag{2.40}$$

where $\lambda > 0$*, and the density is zero, if* $x < 0$ *(see [36]).*

Example 2. *Let* X *be a random variable following an exponential distribution* $X \sim Exp(\lambda)$*. Then, the quantile function of* X *is (see [36])*

$$Q_X(p) = \begin{cases} -\infty, & if\, p = 0 \\ -\ln(1-p)/\lambda, & if\, p > 0 \end{cases} \tag{2.41}$$

We will create $X \sim Exp(\lambda)$ for the different values of $\lambda = 1, 2, 5, 10$.

After we solve the equations (2.23), (2.24), (2.25) and (2.26) for the quantile function $Q_X(p) = -\ln(1-p)/\lambda$, we get the following solutions:

$$m_1 = \frac{-2\ln(p_1 + p_2)}{\lambda} \tag{2.42}$$

$$m_1 + m_2 = \frac{1 - \ln(p_2)}{\lambda} \tag{2.43}$$

Definition 2.5. *The one-parameter Pareto distribution, denoted as $X \sim Pa(\theta)$ is a continuous probability distribution characterized by its shape parameter θ and defined by the cumulative distribution function:*

$$P(X > x) = (1 + x)^{-\theta}, \quad x \geq 0 \tag{2.44}$$

where $\theta > 0$ is the shape parameter (see [15]).

By calculating the inverse of the cdf we can find the quantile function $Q_X(p)$ of the one-parameter Pareto distribution is given by:

$$Q_X(p) = p^{-\frac{1}{\theta}} - 1, \quad 0 < p \leq 1 \tag{2.45}$$

where θ is the shape parameter.

In the research we used the different values of $\theta = 1, 2, 3, 5$

Again after we solve the equations (2.23), (2.24), (2.25) and (2.26) for the $Q_X(p) = p^{-\frac{1}{\theta}} - 1$, we get the following solutions:

$$m_1 = 2((1 - (p_1 + p_2))^{-\frac{1}{\theta}} - 1) \tag{2.46}$$

$$m_1 + m_2 = \frac{\theta}{(\theta - 1)\, p_2} \left(1 - (1 - p_2)^{\frac{\theta - 1}{\theta}}\right) - 1 \tag{2.47}$$

$$\tag{2.48}$$

3 Results

In risk analysis and management, comparing risk measures with the Value-at-Risk is very important. It provides a threshold for risk assessment, indicating the point beyond which losses are expected to occur with a specific likelihood. We gain valuable information into the weaknesses or advantages of the different strategies by comparing alternate risk measures with VaR. We can identify scenarios in which the alternative measures provide a better risk assessment when comparing risk measures with VaR, especially in extreme and tail risk scenarios.

Additionally, by comparing the new risk measures with VaR, we can point out the precise areas where they perform good and those they may fail, supporting professionals in making informed decisions for efficient risk management strategies. Thus the graphical illustrations that we provide in this section will contain VaR so that we can compare the quantization methods and experiments.

3.1 Two Point Quantization

The results of the two point distribution analysis for the P&L values are presented in this section. The VaR predictions and associated probabilities for the loss m and zero-loss scenario are shown in the tables below. We provide the VaR, the probability of the no loss scenario p_0 and its associated value m_0, as well as the probability p_X of the loss m_X for each business date. The Table 3.1 provides the results for two point distribution without any constraint. The first observation is whether m_X values corresponds to moderate risk or which quantile they usu-

ally represent. After checking the mean values of the negative values for each business day, m_X values usually equals to almost double the of the mean of the corresponding negative values. Further exploration reveals that these magnitudes frequently align with quantile ranges spanning the 18^{th} to 22^{nd} percentiles of the whole distribution which indicates m_X represents slightly more than a moderate risk but not an extreme risk, since the magnitude of m_X values always much less than magnitude of VaR.

Date	VaR	m_0	p_0	m_X	p_X
9.08.2022	-16,616,850.79	0	84.00%	-8,676,690.91	16.00%
10.08.2022	-16,148,160.42	0	82.00%	-9,465,722.81	18.00%
11.08.2022	-13,481,350.94	0	82.00%	-7,194,371.27	18.00%
...	...	...	...	...	...
19.06.2023	-28,220,981.58	0	78.00%	-12,311,082.3	22.00%
20.06.2023	-28,507,001.52	0	81.00%	-14,541,955.04	19.00%
21.06.2023	-27,469,711.86	0	81.00%	-11,961,379.04	19.00%

Table 3.1: Two Point Distribution without Constraints Results

Date	VaR	m_0	p_0	m_X	p_X
9.08.2022	-16,616,850.79	0	68.00%	-5,434,526.13	32.00%
10.08.2022	-16,148,160.42	0	67.00%	-4,935,877.99	33.00%
11.08.2022	-13,481,350.94	0	67.00%	-4,394,608.61	33.00%
...	...	...	...	...	...
19.06.2023	-28,220,981.58	0	64.00%	-9,375,190.85	36.00%
20.06.2023	-28,507,001.52	0	65.00%	-10,167,474.9	35.00%
21.06.2023	-27,469,711.86	0	66.00%	-9,025,366.24	34.00%

Table 3.2: Two Point Distribution with Mean Constraint Results

On the other hand, the Table 3.2 shows the results for two point distribution with mean constraint experiment we conducted which is mentioned in the Section 2.3.1. The introduction of the mean constraint appear to create a trade-off between mean preservation and propensity for losses. However, it is worth noting that while the mean constraint contributes to a more moderated risk level, there exists a slight variance between the mean of the newly formed two point distribution and the mean of the original distribution. This difference highlights that, although the constraint influences the risk representation, it could not achieve an exact alignment between the two means. Nevertheless, the introduction of the constraint has succeeded in reshaping the risk distribution to a form that makes m_X closely approximates the mean of

the negative values, which makes the m_X values more moderate with higher propensity. The choice between the two approaches may depend on the specific risk tolerance and objectives of the institution. The first table (the Table 3.1) offers a broader representation of potential loss scenarios, while the second table (the Table 3.2) aligns more closely with the mean, which may be preferred in certain risk management strategies.

Date	VaR	m_0	p_0	m_X	p_X
9.08.2022	-16,616,850.79	0	92.00%	-19,482,192.6	8.00%
10.08.2022	-16,148,160.42	0	91.00%	-21,130,078.86	9.00%
11.08.2022	-13,481,350.94	0	91.00%	-13,452,836.16	9.00%
...	...	...	...	...	...
19.06.2023	-28,220,981.58	0	89.00%	-27,007,281.37	11.00%
20.06.2023	-28,507,001.52	0	81.00%	-20,438,810.59	19.00%
21.06.2023	-27,469,711.86	0	91.00%	-46,667,387.32	9.00%

Table 3.3: Two Point Distribution with Mean and Variance Constraint Results

The Table 3.3 provides the results for two point distribution with mean and variance constraints for the second experiment mentioned in the Section 2.3.1. The results provide a conservative approach to quantifying risk, where mean and variation are strictly controlled. The magnitude of m_X values increased and p_X percentage decreased significantly. Moreover when we see some spesific examples such as the business day 21.06.2023, the m_X value act as an outlier. The minimum value of that day, the highest magnitude of the losses, is -31,253,164.73 however the calculated m_X value is -46,667,387.32. This points out that implementing two constraints at the same time deconstructed the optimization problem.

3.1.1 Comparison of m_X with Value-at-Risk

A dynamic representation of risk evolution over a range of business days is shown in the time series graph. The x-axis denotes the chronological progression of business days, while the y-axis corresponds to the magnitude of losses. The plotted points on the graph consist of two key components which are VaR values and m_X values. As the graph extends along the x-axis, the fluctuating VaR values highlight the changing risk exposure over time.

In the Graph 3.1, which is that case of two point distribution without constraints, we can see that m_X values following the same trend as VaR.This alignment between m_X and VaR values suggests that the chosen risk measure is efficient in capturing and reflecting the underlying risk dynamics.

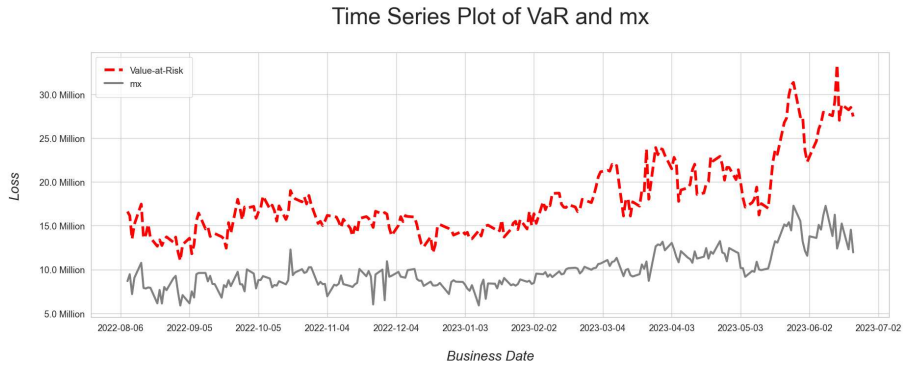

Figure 3.1: Two point distribution without constraints time series graph

In the Graph 3.2, a distinct pattern emerges from the comparison between the original two-point distribution and its constrained version. Remarkably, the trend in the m_X values, which represented the magnitude of losses, exhibits a delicate deviation from the VaR values due to the application of the mean constraint. Frequently sharp movements of the risk values is observed, as we can see from the sudden peaks throughout the business days, instead of a more stable values.

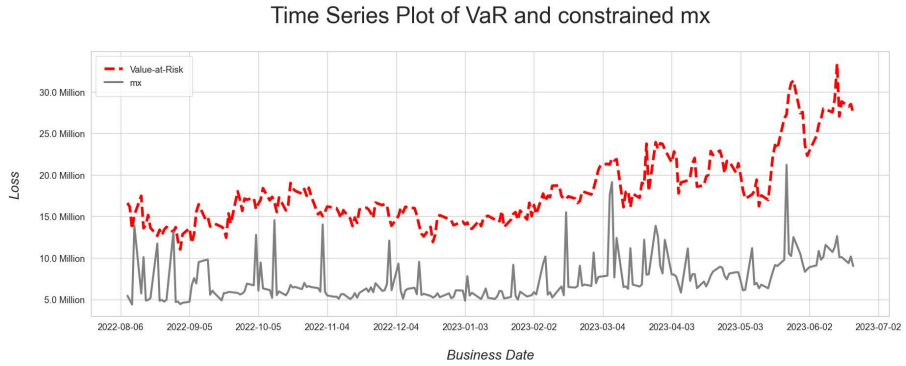

Figure 3.2: Two point distribution with mean constraint time series graph

The Graph 3.3 indicates a dynamic risk pattern resulting from the joint application of mean and variance constraints to the two-point distribution. The constrained approach leads to sharper and more frequent shifts in the quantified risk levels over the observed business days as we see in the results in the Table 3.3. It can be seen how much the m_X values fluctuate. Another observation is unlike the previous cases where m_X consistently remained below VaR, this constrained version witnesses instances where m_X surpasses VaR.

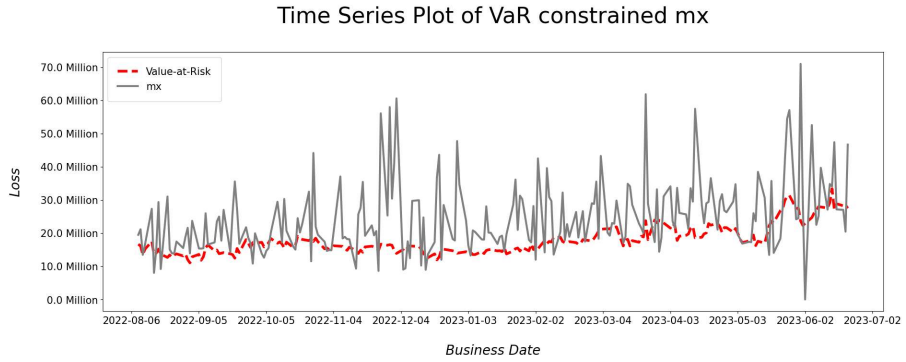

Figure 3.3: Two point distribution with mean and var constraints time series graph

3.1.2 Analysis of the original and new distributions

The graph created provides a representation of the original P&L distribution and the new distribution. Since the original distribution is a continuous distribution, the bell-shaped smoothed probability density function curve is created. The VaR values for each business day provides an important reference points for assessing risk alongside the curve. These VaR values are set at a level where the probability of losses occurring is 1. And then finally we have the points representing the new distribution which are (m_X, p_X) and $(0, 1 - p_X)$

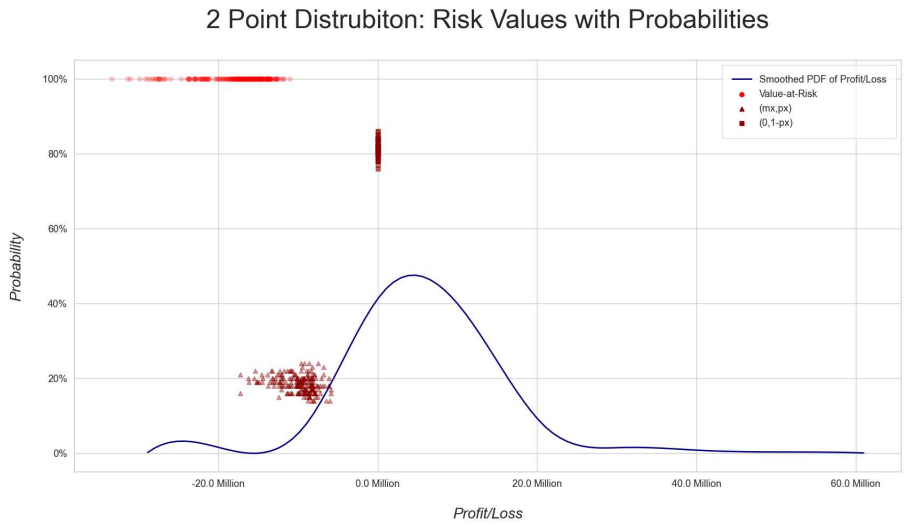

Figure 3.4: Two Point Distribution without constraint PDF graph

In the Graph 3.4 it is clear that the clustering of points in the graph signifies a relatively consistent risk profile, where the distribution is compact. Conversely, in the Graph 3.5 the spreading

of points in the graph suggests a wider range of potential risk scenarios, indicative of a higher level of variability in the risk values. In particular, some m_X values have been assigned noticeably high probabilities, which was not experienced with the unconstrained version. And it is not preferred to have a low magnitude of m_X value with high propensity which is very close to the point $(0, 1-p_X)$. The aim is to find two points that can represent the whole. The transformation from a clustered point representation to a more spread representation signifies that the mean constraint has introduced an element of variability that was absent in the unconstrained distribution.

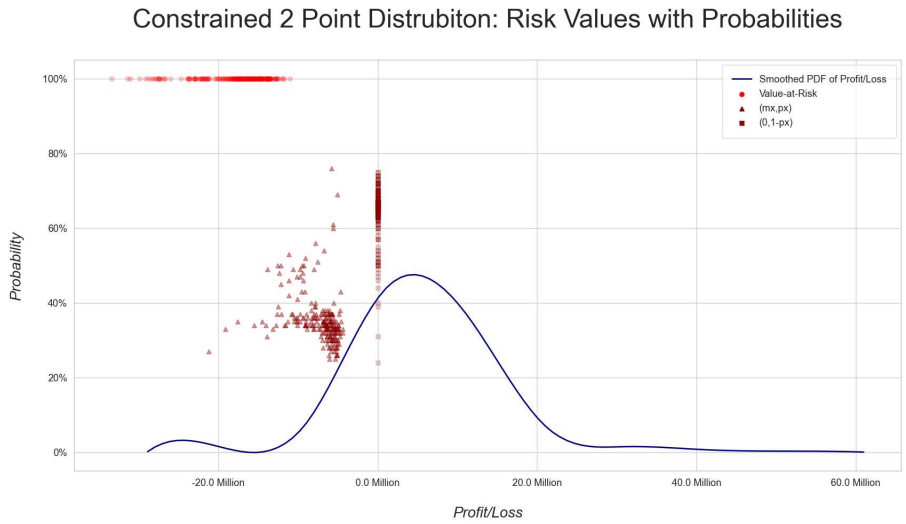

Figure 3.5: Two point distribution with mean constraint PDF graph

The spreading of points in the Graph 3.6 is even more clear compared to both Graph 3.4 and Graph 3.5. This suggests that the addition of variance constraints to the distribution has introduced further variability into the risk profile. The wider distribution of points across the magnitude values indicates a wider range of possible risks.Unlike in the Graph 3.5 where certain m_X values had notably high probabilities, the Graph 3.6 presents a more balanced distribution of probabilities across the risk magnitudes. Although the probabilities fluctuate across the distribution, they do not show unusually high peaks. Also in the Graph 3.5 we see the spread causing low magnitude of m_X points however in the two constraint version it is the opposite.

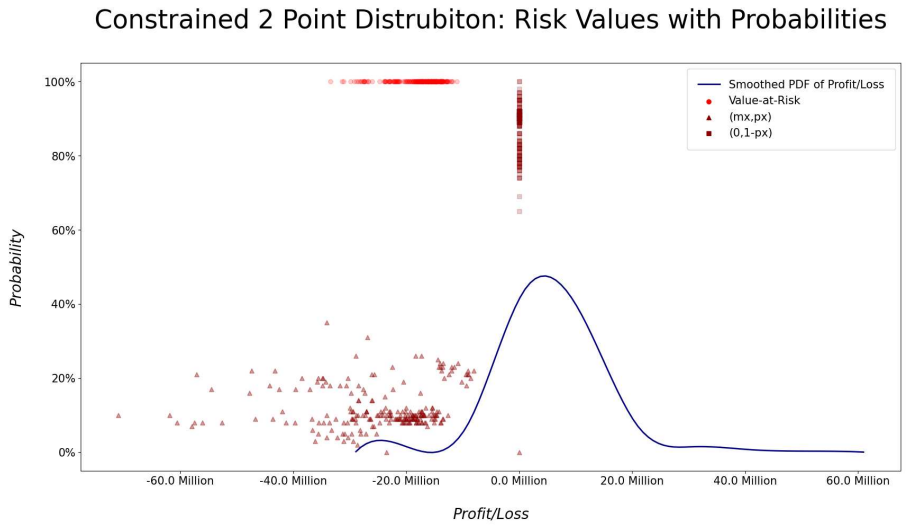

Figure 3.6: Two point distribution with mean and var constraints PDF graph

3.2 Three Point Quantization

In this section we will be using the same graphical visualization as in the Section 3.1. In addition to that we're going to show the results of the experiment of different distributions with synthetic data.

3.2.1 Synthetic Data for Different Quantile Functions

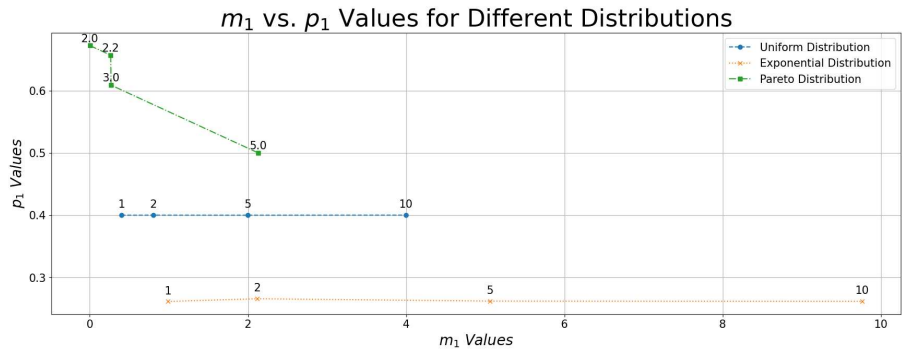

Figure 3.7: Magnitude-propensity plots for m_1 and p_1 values of Uniform Distribution $U(0, a)$, Exponential Distribution $Exp(\lambda)$ and Pareto Distribution $Pa(\theta)$

After creating the synthetic data with the parameters described in the Section 2.4.4, the Figure 3.7 and Figure 3.8 is created to see the changes of each magnitude between distributions

with different parameters. In the Figure 3.7 we can see that both uniform and exponential distributions have constant propensity. Their propensity stayed same after the change of the parameters. For the uniform distribution, this behavior can be explained by the definition of the uniform distribution given in the Section 2.4.4. In a uniform distribution $U(0, a)$, all outcomes within the interval (0, a) are equally likely. Therefore, regardless of the specific value of a, the propensity of outcomes falling within the quantization threshold remains the same. Because we are not changing the number of samples the distribution has instead we're changing the range of values. However, as a increases, the range of possible values expands, leading to higher magnitude values (m_x). This is because there is a greater spread of values within the distribution, some of which may be larger in magnitude. For the exponential distribution as parameter λ increases the distribution becomes more concentrated around zero which causes m_X to be larger. In general Pareto distribution has lower magnitude with higher propensity. And the increment of the shape parameter θ resulted with higher magnitudes with higher propensity. As θ increases, the distribution's tail becomes heavier, leading to potentially extreme values. However the expected outcome would be the decrease in propensity values.

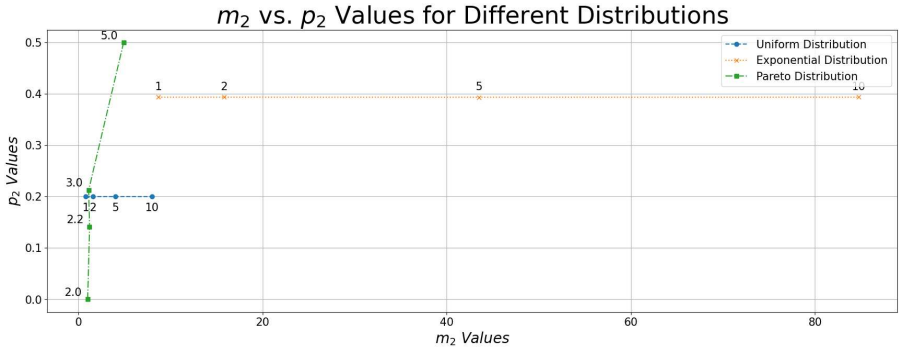

Figure 3.8: Magnitude-propensity plots for m_2 and p_2 values of Uniform Distribution $U(0, a)$, Exponential Distribution $Exp(\lambda)$ and Pareto Distribution $Pa(\theta)$

On the other hand in the Figure 3.8 p_2 remains constant in the uniform distribution and exponential distribution just like in the previous case (p_1). In the uniform distribution and pareto distribution m_2 have higher magnitude with less propensity which is an expected scenario. However for the exponential distribution, unlike the uniform distribution, both m_2 and p_2 are higher than m_1 and p_1. For the pareto distribution higher values of the shape parameter θ, both m_2 and p_2 are higher, indicating a higher likelihood of extreme values with larger magnitudes since the tail of the distribution becomes heavier.

3.2.2 Results of the Three Point Quantization

The results for three point distribution offers a comprehensive information into the risk quantification. The values presented in the tables indicates the distribution of potential losses across different magnitudes. Three distinct m values (m_0, m_1, m_2) are given by their corresponding probabilities (p_0, p_1, p_2). The m values represent different levels of potential losses, while the p values provide the probabilities associated with these loss values.

Date	VaR	m_0	p_0	m_1	p_1	m_2	p_2
9.08.2022	-16,616,850.79	0	76.00%	-5,857,602.68	21.00%	-17,136,050.75	3.00%
10.08.2022	-16,148,160.42	0	71.00%	-5,353,215.68	24.00%	-13,996,210.08	5.00%
11.08.2022	-13,481,350.94	0	72.00%	-4,010,364.98	22.00%	-10,466,383.81	6.00%
...	...	...	...	...	...	...	...
19.06.2023	-28,220,981.58	0	70.00%	-9,374,225.23	25.00%	-23,018,215.94	5.00%
20.06.2023	-28,507,001.52	0	71.00%	-9,168,486.97	24.00%	-22,617,174.73	5.00%
21.06.2023	-27,469,711.86	0	65.00%	-7,433,802.8	28.00%	-19,744,136.47	7.00%

Table 3.4: Three Point Distribution without constraint results

In the Table 3.4, representing the Three Point Distribution without constraint, several key trends can be observed. The inclusion of the third magnitude m_2 and its probability p_2 expand the risk range. While the probability values for m_2 are relatively lower, they signify the occurrence of even more extreme risk events that have a significant impact on the overall risk assessment. In this case m_1 values representing moderate risk by acted like a almost mean of the negative values in the distribution.

Date	VaR	m_0	p_0	m_1	p_1	m_2	p_2
9.08.2022	-16,616,850.79	0	75.00%	-5,363,846.0	22.00%	-21,980,696.79	3.00%
10.08.2022	-16,148,160.42	0	71.00%	-5,510,737.68	27.00%	-21,658,898.1	2.00%
11.08.2022	-13,481,350.94	0	75.00%	-4,981,025.38	23.00%	-18,462,376.32	2.00%
...	...	...	...	...	...	...	...
19.06.2023	-28,220,981.58	0	71.00%	-10,081,949.19	27.00%	-38,302,930.77	2.00%
20.06.2023	-28,507,001.52	0	73.00%	-10,302,648.16	26.00%	-38,809,649.68	2.00%
21.06.2023	-27,469,711.86	0	69.00%	-8,949,891.35	30.00%	-36,419,603.21	2.00%

Table 3.5: Three Point Distribution with VaR constraint results

The values of m_2 in the Table 3.5 demonstrates a shift towards greater magnitudes compared to the Table 3.4. This shift is a direct result of the introduced constraint, which enforces a more conservative perspective on extreme potential losses. It can be seen that increasement of the

magnitude of m_2 did not shift the magnitude of m_1 so the general structure of the approach still holds. In addition to the shift in magnitude, the probabilities (p_0, p_1, p_2) in the Table 3.5 are adjusted to ensure that the probabilities align with the constraint while maintaining their structure. There is no outlier seen from the table.

3.2.3 Comparison of m_1 and m_2 with Value-at-Risk

Similar to two point distribution time series graphs are shown in the Figure 3.9 and Figure 3.10. This time the graph has m_1 and m_2 values with also VaR as before througout the business days. Within this graph, several crucial elements are depicted for each business day.

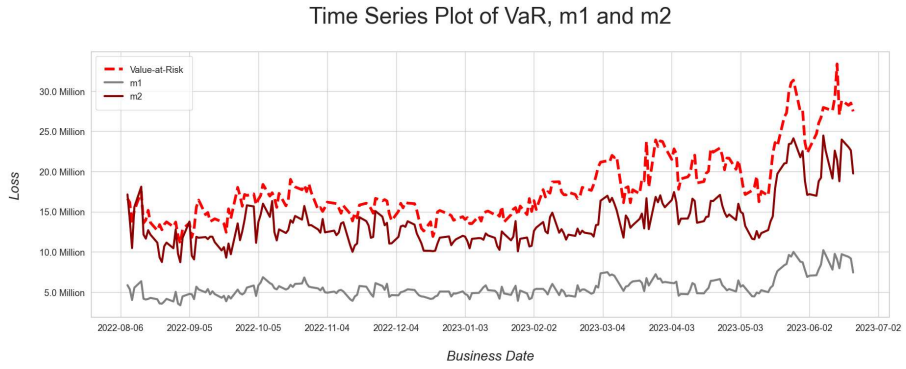

Figure 3.9: Three point distribution without constraints time series graph

The Graph 3.9 reveals a clear trend in the behavior of m_1 and m_2 values over time. Both m_1 and m_2 generally follow a similar behaviour as the VaR values. This indicates that these potential loss levels are sensitive to the market conditions and risk factors that are also impacting the VaR. The graph also illustrates that, with the exception of four points, m_2 values predominantly remain below the VaR values. On the other hand, m_1 appears to act as a moderate risk indicator as previously stated. It generally follows the VaR trend but maintains a distinct margin from it.

The most notable observation in the Graph 3.10 is the preservation of the trends in the magnitudes m_1 and m_2. Unlike the two point distribution with constraints, where significant fluctuations occurred due to the constraint implementation, the trends for both m_1 and m_2 remain relatively stable in this graph. This stability indicates that the VaR constraint has not induced major volatility in the potential loss levels. It can be seen that the VaR constraint has successfully altered the relationship between m_2 and the VaR.

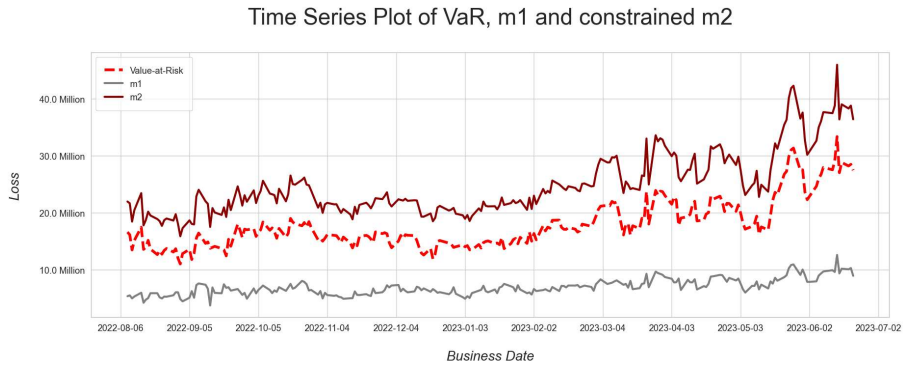

Figure 3.10: Three point distribution with VaR constraint time series graph

3.2.4 Analysis of the original and new distributions

Similar to the Section 3.1.2, the original distribution and the VaR values presented with the same logic as before. The smoothed probability density function curve retains its characteristic bell shape. Additionally, the graph incorporates the points $(0, 1 - p_1 - p_2)$, (m_1, p_1) and (m_2, p_2) from the new distribution for each business day which corresponds to no loss, moderate and extreme risk points, respectively.

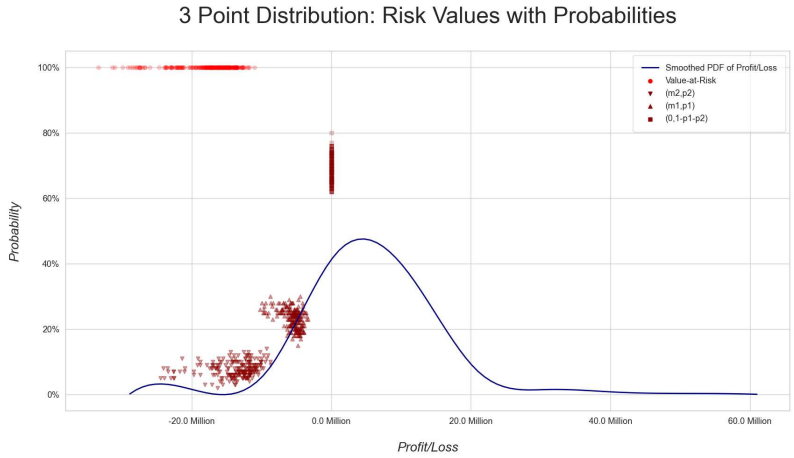

Figure 3.11: Three point distribution without constraints PDF graph

It can be observed in the Figure 3.11 that while the m_1 cluster forms a relatively compact and concentrated group, the m_2 values exhibit slightly more variability within their cluster. This indicates that the potential losses associated with m_2 are more distributed than those of m_1, considering a higher level of unpredictability.

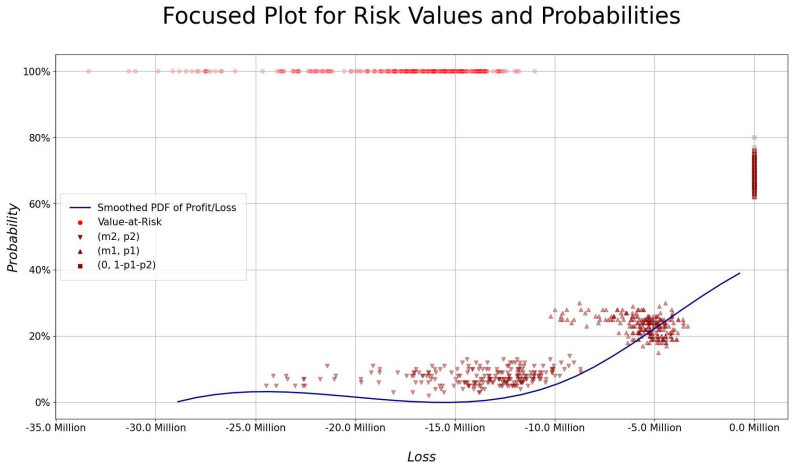

Figure 3.12: Three point distribution without constraints focused PDF graph

In the Figure 3.12, three point distribution without constraints focused PDF graph narrows the analysis to the negative segment of the smoothed PDF curve, enabling a detailed exploration of potential losses within the context of the three point distribution. So that the findings we conclude before, such as m_2 range, can be seen clearly. m_2 values range between -7 million to -25 million.

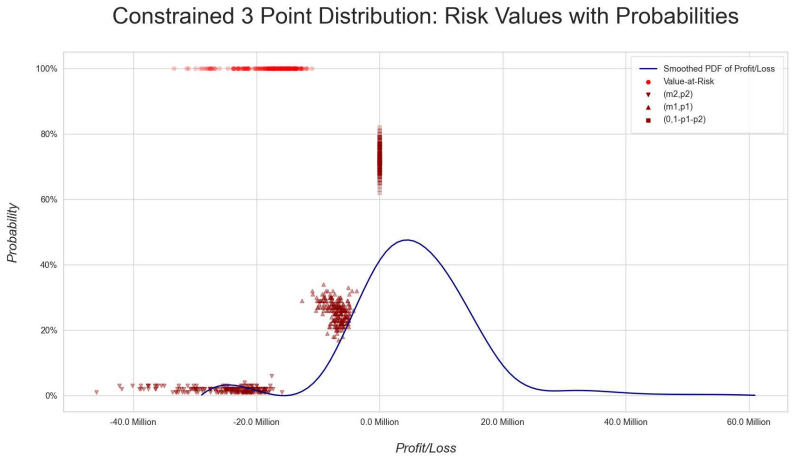

Figure 3.13: Three point distribution with VaR constraint PDF graph

The impact when introducing a VaR restriction to the three point distribution is shown in the Figure 3.13. The range of m_2 values continues to reveal diversity, by considering different potential loss magnitudes. However, a notable difference lies in the stability of the associated probabilities. While these probabilities remain consistently low, the constraint has effectively

confined their fluctuations. The characteristics of m_1 remain consistent, indicating moderate risks.

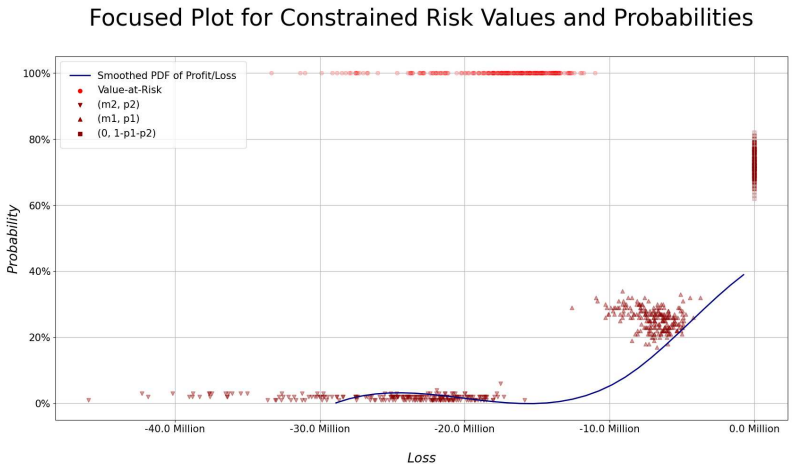

Figure 3.14: Three point distribution without constraints focused PDF graph

In the Figure 3.14, an important transformation is observed in the (m_2, p_2) point. With the constraint $|m_2| > |VaR|$, the range of m_2 extends from -15 million to greater than -40 million, showing an expanded span of extreme risk magnitude. This specific adjustment underscores the impact of the constraint on the evaluation of extreme risk scenarios within the risk profile.

4
Conclusion

The previous chapters provided clarity on many aspects of risk measurement, ranging from traditional approaches to innovative approaches, as we explore the complexities of risk analysis and management. We have started out with better understand the Faugeras and Pagès's magnitude propensity approach by implementing on a real world dataset then experimenting with the constraint implementation which was not mentioned in their paper. After having the enough background, we created the extended version of Faugeras and Pagès's paper, three point quantization. The theoretical analysis is more complex than the two point quantization however we achieved the sufficient conditions for the extended version we created. Before the implementation of the real world dataset and the constraint experiments again implemented, synthetic data of the uniform distribution, exponential distribution and pareto distribution is conducted.

In this final chapter, we summarize our findings, offer perceptive explanations of the findings, highlight the advantages and limitations of the suggested technique, and chart the way for further research.

4.1 Interpretation of the results

The exploration of different risk quantification techniques has yielded useful information into the financial risk world. The graphical analysis of the two point distribution, which is Faugeras and Pagès's work, illuminated a significant relationship between VaR values and (m_X, p_X)

points. Since all of our analysis include VaR we reveal a parallel trend and highlight the integral role of VaR as a threshold for risk assessment. This trend further resonated in the two point distribution with two different constraint experiments. The experiments we conducted showed that the mean and variance constraints broke the integrity of the new distribution. When we added these constraints, the stability was disrupted, causing the distribution to fluctuate which their effectiveness in risk assessment. An ideal risk measure should be intuitive, stable, easy to compute, easy to understand, coherent and interpretable in economic terms (see [10]). It means that small changes in model parameters should not produce large changes in the estimated loss distribution and the risk measure. Therefore the constrained version is not an ideal risk measure we are looking for.

The implementation of three point distribution resulted in smooth integration of (m_1, p_1) and (m_2, p_2) points into the risk environment. The extended approach successfully created and implemented to have the three point representation of the loss distribution. The subsequent exploration of the three point distribution with a VaR constraint reinforced the distinct characteristics of extreme risk scenarios, as highlighted by the enhanced (m_2, p_2) points that exceeded the VaR threshold. Unlike to the constrained version of two point distribution, the extended version stayed stable showing an ideal characteristic of a risk measure. Moreover the uniform distribution, exponential distribution and pareto distribution experiment allowed us to assess how changes in distribution and also its parameters impacted the created risk measure. As expected, both the uniform and exponential distributions maintained constant risk propensity while exhibiting increased risk magnitudes as distribution parameters were altered. On the other hand, the Pareto distribution displayed higher magnitudes with lower risk propensity.

4.1.1 Overlapping Rate

A fundamental criterion for assessing the effectiveness of risk measures is their stability over time as mentioned in the beginning of the Section 4.1. A robust risk measure should consistently capture the potential variability and uncertainties in a financial system. Thus we created a statistical analysis that underscores this stability is the calculation of an 'overlapping rate' among different magnitude measures.

This concept offers valuable information into the degree of alignment or convergence between various risk scenarios. Basically, the overlapping rate measures the extent to which adjacent magnitudes in a risk measure distribution intersect or overlap with each other. By quantifying the percentage of overlapping between adjacent risk measures, we gain a deeper under-

standing of how these measures behave within their respective ranges. For example, given a distribution with multiple magnitude measures, such as m_1 and m_2, we can calculate the percentage of overlapping between m_1 and m_2, shedding light on their coherence and potential range convergence. This analysis improves our understanding of the risk dynamics and helps in assessing the reliability of risk measures.

Definition 4.1. *Let $m, n \in \mathbb{N}$, and let m_n_values, m_t_values be the list of points of the new risk measure. Denote*

$$R(m_n\_values) = \textit{range}\left(\min(m_n\_values), \max(m_n\_values)\right) \tag{4.1}$$

as the range of m_n.

The overlapping rate function, denoted $OR(m_n\_values, m_t\_values)$, is defined as:

$$OR(m_n\_values, m_t\_values) = \frac{\sum_{m_t \, in \, m_t\_values} \delta_{m_t}(R(m_n))}{len(m_t\_values)} \times 100 \tag{4.2}$$

where len(m_t_values) means the total number of values in m_t_values.

The computed overlapping rate between m_1 and m_2 within the three point distribution stands at %4.87. This indicates that there is a modest level of overlap between the adjacent magnitudes of m_1 and m_2. Such an overlapping rate implies that while m_1 and m_2 shows some degree of convergence within their respective ranges but they also retain a distinct separation. This finding underscores the inherent dynamics of the risk scenario represented by the three point distribution. Particularly, a higher overlapping rate could suggest a more clear convergence, whereas a lower rate points to a greater difference between adjacent risk measures.

Intriguingly, the constrained three point distribution exhibits an overlapping rate of %0 between m_1 and m_2. This result suggests a clear change from the three point distribution, indicating a minimal to nonexistent alignment between these two adjacent magnitudes. The %0 overlapping rate underscores the impact of the imposed constraints, which appear to have led to a more distinct and isolated behavior between m_1 and m_2. This outcome may imply that the constraints have effectively reduced the potential for convergence between these risk measures, resulting in a more diversified distribution of outcomes.

4.2 Strengths and limitations of the proposed methodology

The exploration of risk quantification approach introduced by the Faugeras and Pagès' and extending it with experiments revealed several notable strengths, as well as limitations. The following arguments can be interpreted as strengths of the proposed three point quantization:

- Comprehensive Risk Profiling: three point quantization approach provides a more complete view of risk profiles than the two point quantization by offering both moderate and extreme risks. However both of them allow for a dynamic representation of risk scenarios, considering both magnitude and propensity, thus enabling a more refined understanding of potential losses.
- Visualization: The visual representations offered by the graphs facilitate effective communication of risk scenarios. The distribution of potential losses, VaR thresholds, and the impact of various constraints can be easily understood.
- Identification of Extreme Risks: The incorporation of constraints, such as the VaR constraint, sharpens the focus on extreme risk scenarios. This helps to identify the critical risk thresholds and the assessment of vulnerabilities associated with unexpected events.
- Flexibility in Constraint Implementation: The methodology has successfully achieved implementing the VaR constrained which providing the flexibility to align risk quantification with particular business contexts.

However there are also some limitations that should be taking into account:

- Sensitivity to Data Quality: The accuracy of the risk quantification heavily relies on the quality and completeness of the underlying data. Inaccurate or incomplete data may lead to biased or unreliable results, affecting the integrity of risk assessments.
- Assumption Dependence: The methodology's effectiveness is based on the appropriateness of assumptions made during the distributional modeling. Deviations from real-world conditions may impact the reliability of the information generated.
- Complexity of Interpretation: While the graphical representations improves understanding, interpreting the interactions of different points, thresholds, and constraints might pose challenges theoretically, especially for non-experts in the field of risk management. In the Section 2.4.3 we have encountered the challenge of mathematical computation due to the complexity.

Hence the proposed methodology presents a valuable framework for risk quantification, offering comprehensive insights into risk environment and helping decision-making processes. These information pave the way for future research directions aimed at refining and expanding the applicability of risk quantification techniques.

4.3 Future research directions

The methodology employed in this study opens up several promising paths for future research, aiming to improve the robustness, applicability, and versatility of risk quantification techniques.

One of the most convenient direction is the extension to higher-dimensional. Building on the foundation of the two point and three point distributions, a natural progression is the exploration of higher-dimensional distributions. For instance, the incorporation of a five point distribution could allow for a finer differentiation of risk scenarios. In this context, (m_3, p_3) could represent moderate risks, while (m_4, p_4) could signify extreme the profit or loss scenarios. This extension would offer a more refined and accurate representation of risk profiles including profit scenarios. To be more clear the higher dimensional distribution can be defined as,

$$P^Y = (1 - p_1 - p_2 - p_3 - p_4)\delta_0 + p_1\delta_{m_1} + p_2\delta_{m_2} + p_3\delta_{m_3} + p_3\delta_{m_3} \tag{4.3}$$

where $|m_1| < |m_2|$ and $|m_3| < |m_4|$.

Also another research can be implemented for the incorporation of external factors. Future research could investigate the integration of external factors, such as macroeconomic indicators or geopolitical events, into the risk quantification framework. By accounting for these factors, the methodology could provide a more comprehensive assessment of potential risk exposures, improving the predictive power of the analysis.

Lastly adapting to contexts to specific industry might give a clear and specific aspect. The methodology's flexibility allows for adapting to specific industries and sectors. Future research could focus on customizing the approach to address the unique risk scenarios of various sectors, such as healthcare, energy, or technology.

In conclusion, the proposed methodology serves as a stepping stone for advancing the field of risk quantification. By extending the approach to higher-dimensional distributions, incorporating external factors, and embracing innovative technologies, researchers can unlock new insights and applications in risk analysis, ultimately empowering decision-makers to make more informed and proactive choices in managing and mitigating risks.

References

[1] Acerbi, C. Spectral measures of risk: A coherent representation of subjective risk aversion. *Journal of Banking and Finances 26*, 7 (2002), 1505–1518.

[2] Acerbi, C., and Tasche, D. Expected shortfall: a natural coherent alternative to value at risk. *Economic Notes 31*, 2 (2001), 379–388.

[3] Acerbi, C., and Tasche, D. On the coherence of expected shortfall. *Journal of Banking and Finances 26*, 7 (2002), 1487–1503.

[4] Agency for Healthcare Research and Quality. 2013 annual hospital-acquired condition rate and estimates of cost savings and deaths averted from 2010 to 2013, 2013.

[5] Allen, F., . B. T. G. Systemic risk and macroeconomic resilience. *Journal of Financial Economics 97* (2010), 470–487.

[6] Artzner, P., Delbaen, F., Eber, J. M., and Heath, D. Coherent measures of risk. *Mathematical Finance 9*, 3 (1999), 203–228.

[7] Balbás, A., Garrido, J., and Mayoral, S. Properties of distortion risk measures. *Methodol Comput Appl Probab 11* (2009), 385–399.

[8] Bank for International Settlements. International convergence of capital measurement and capital standards: A revised framework, 2006.

[9] Basel Committee on Banking Supervision. *Fundamental Review of the Trading Book: A Revised Market Risk Framework*. 2013. Online.

[10] Basel Committee on Banking Supervision (BCBS). Range of practices and issues in economic capital frameworks. Bank For International Settlements, March 2009.

[11] Danielsson, J. *Financial Risk Forecasting: The Theory and Practice of Forecasting Market Risk with Implementation in R and Matlab*, 1st ed. Wiley, 2011.

[12] Dowd, K. *Measuring Market Risk*, 2nd ed. John Wiley & Sons, 2007.

[13] Embrechts, P., Puccetti, G., and Rüschendorf, L. Model uncertainty and var aggregation. *Journal of Banking & Finance 37*, 8 (2013), 2750–2764.

[14] European Securities and Markets Authority (ESMA). Final report: Guidelines on liquidity stress testing in ucits and aifs, 2020.

[15] Faugeras, O., and Pagès, G. Risk quantization by magnitude and propensity. *Quantitative Finance* (2021). Available at SSRN: https://ssrn.com/abstract=3854467 or http://dx.doi.org/10.2139/ssrn.3854467.

[16] Fender, I., Gibson, M. S., and Mosser, P. C. An international survey of stress tests. *Federal Reserve Bank of New York Economic Policy Review 7*, 10 (November 2001).

[17] Fissler, T., Ziegel, J. F., and Gneiting, T. Expected shortfall is jointly elicitable with value at risk – implications for backtesting. *arXiv preprint arXiv:1507.00244* (2015).

[18] Graf, S., . L. H. *Foundations of Quantization for Probability Distributions*, 1st ed. 2000.

[19] Horn, R. A., and Johnson, C. R. *Matrix Analysis*, 2nd ed. Cambridge University Press, 1985.

[20] Hull, J. C. *Risk Management and Financial Institutions*, 6th ed. Wiley, 2018.

[21] Jorion, P. *Value at Risk: The Benchmark for Managing Financial Risk*, 3rd ed. McGraw-Hill, 2000.

[22] LexisNexis Risk Solutions. Lexisnexis u.s. home insurance trends report, 2021.

[23] Lloyd, S. P. Least squares quantization in pcm. *IEEE Transactions on Information Theory 28*, 2 (1982), 129–137.

[24] Malz, A. M. *Financial Risk Management: Models, History, and Institutions*. John Wiley Sons, Inc., New Jersey, 2011.

[25] McNeil, A. J., Frey, R., and Embrechts, P. *Quantitative Risk Management: Concepts, Techniques, and Tools*, 1st ed. Princeton University Press, 2005.

[26] Novelli, R. Bollettino statistico. *Istituto per la Vigilanza sulle Assicurazioni (IVASS)* (2016-2021).

[27] Pagès, G., Papanicolaou, G., and Sircar, R. A mathematical approach to hedging and risk management with constant elasticity of variance (cev). *Applied Mathematical Finance 11*, 3 (2004), 211–228.

[28] Panaretos, V., and Zemel, Y. Statistical aspects of wasserstein distances. *Annual Review of Statistics and Its Application 6* (2019), 405.

[29] Pichler, A., and Shapiro, A. Mathematical foundations of distributionally robust multistage optimization. *SIAM Journal on Optimization 31*, 4 (2021), 3044–3067.

[30] Pishro-Nik, H. *Introduction to Probability, Statistics, and Random Processes*. Kappa Research LLC, 2014.

[31] Pritsker, M. G. The hidden dangers of historical simulation. FEDS Discussion Paper No. 2001-27.

[32] Rachev, S. T., and Rüschendorf, L. *Mass Transportation Problems*, vol. Vol. I of *Probability and its Applications (New York)*. Springer-Verlag, 1998.

[33] Rejda, G. E., and McNamara, M. *Principles of Risk Management and Insurance*, 13th ed. Pearson, 2016.

[34] Rudin, W. *Real and Complex Analysis*, 3rd ed. McGraw-Hill, 1987.

[35] Salamon, D. A. *Measure and Integration*. ETH Zürich, August 2020.

[36] Soch, J., Faulkenberry, T. J., Petrykowski, K., and Allefeld, C. The book of statistical proofs. `https://doi.org/10.5281/zenodo.4305950`, 2020. Version 2020.

[37] Villani, C. *Optimal Transport: Old and New*, vol. 338 of *Grundlehren Math. Wiss.* Springer, 2008.

[38] Zabolotskyy, T. Estimation of confidence level for value-at-risk: statistical analysis. *Economic Annals-XXI 158*, 3-4(2) (2016), 83–87.

Acknowledgments

I would like to express my deepest appreciation to all of the amazing people who have supported me throughout my journey. Michele Bonollo's guidance in my professional journey has been invaluable, shaping my growth within the company. I'm also grateful to Martino Grasselli, my university supervisor, for generously dedicating his time and offering insightful feedback on my thesis.

To my incredible mother, Hosnaz Oz, with a heart full of kindness, you have been my guiding light. I will always remember your sacrifices and endless efforts that you did for me. My dearest father, Ismail Oz, you always make me feel special and I love the wonderful bond we have; it's something to be proud of. And to my younger brother, Deniz Oz, you are my best friend. As your older sibling, I find purpose in being the best version of myself for you. I want you to know that my support and presence will forever stand by your side. I love you so much.

During the master's degree, I've had the pleasure of making some wonderful friends who have added so much joy to my journey. Among them, Berke and Rocio hold a special place in my heart. We've shared countless moments of laughter and support, and I look forward to seeing them shine even more. Additionally, I cherish the time spent with Cecilia and Vitor who added a spark in my Milan chapter and I am grateful for having them around.